ON THE ORIGIN AND FUNCTION OF WAXING AND WANING IN PACEMAKER ACTIVITY IN THE SMALL INTESTINE

ON THE ORIGIN AND FUNCTION OF WAXING AND WANING IN PACEMAKER ACTIVITY IN THE SMALL INTESTINE

BY,

ANDREW J PAWELKA HBSc

A Thesis

Submitted to the School of Graduate Studies

in Partial Fulfillment of the Requirements

for the Degree

Master of Science

McMaster University

MASTER OF SCIENCE (2013)
(Medical Sciences)

McMaster University
Hamilton, Ontario

TITLE: On the Origin and Function of Waxing and Waning in Pacemaker Activity in the Small Intestine

AUTHOR: Andrew J Pawelka, HBSc (University of Guelph)

SUPERVISOR: Professor Jan D Huizinga, PhD

NUMBER OF PAGES: xii, 105

ABSTRACT

The small intestine of the gastrointestinal tract displays a variety of motor patterns involved in the mixing, digestion, and propulsion of luminal content. Ultimately, it is the co-ordinated effort of smooth muscle contraction influenced by neural and myogenic stimulation that facilitate these motor patterns. While neural input from the enteric nervous system (ENS) and slow wave producing activity of the peacemaking interstitial cells of Cajal (ICC) in the myenteric plexus (ICC-MP) are key players in the manipulation of smooth muscle cells, the mechanisms behind the onset the segmentation motor pattern are currently unknown.

I have demonstrated with intracellular recordings of electrical activity from circular smooth muscle cells, the same nutrient stimulants used to induce the segmentation motor pattern in whole organ preparations evokes the waxing waning phenomenon of the smooth muscle slow wave. Through the use of continuous wavelet transformation analysis on nutrient induced waxing waning, it was determined that the induction of a rhythmic low frequency component is responsible for the generation of waxing waning.

Stimulated low frequency activity after methylene blue mediated elimination of ICC-MP slow wave activity suggested the low frequency component did not originate from the ICC-MP. The hypothesis emerged that the ICC of the deep muscular plexus (ICC-DMP), on the opposite side of the circular muscle thickness to the ICC-MP, were responsible for the low frequency oscillations. ICC-DMP networks in close physical

proximity to nerve fibers were found to be under tonic inhibited by nitric oxide, and to respond to substance P stimulation. Both alleviation of the inhibition and stimulus by tachykinergic neurotransmission induced the low frequency component and waxing waning.

The ENS and myogenic pacemakers play an important role in stimulating the segmentation motor pattern. ICC-DMP are the pacemakers responsible for generation of the low frequency component involved in waxing waning and segmentation.

AKNOWLEDGEMENTS

Funding for this project was provided by a CIHR operating grant for Dr. Jan Huizinga.

The past two years as a graduate student have been a rewarding experience. It has inspired as well as provided me with the skills required to tread through hardship in order to achieve any and every goal as I move forward in life. The guidance and support I have received from Dr. Jan Huizinga has been priceless and of the utmost importance for my success. For that I am truly grateful. His expertise, passion, and dedication to science have inspired me to strive for greater heights and to approach all endeavours with the same mind-set. I would like to thank Jan for all the opportunities he provided to participate in research, publications, and the genuine interest he showed in the time he took to discuss research and personal issues. I am forever grateful and incredibly fortunate for this experience. This opportunity has been invaluable to my future success.

I would also like to thank the members of my supervisory committee for the guidance they imparted. Experts in their field, Dr. Premsyl Bercik, Dr. Wolfgang Kunze, and Dr. Eva Werstiuk each provided thoughtful suggestions and contributions to my research. I am extremely grateful for the time and effort they afforded into my academic career.

I want to thank all the members of the Huizinga lab, past and present, for providing an enjoyable work environment. I am humbled to have worked with such intelligent and enthusiastic individuals. Specifically, I'd like to thank Dr. Sean Parsons,

Dr. Yong Fang Zhu and Amir Khosdel for the generosity of their time and efforts in teaching me the various techniques I used throughout the development of my thesis. Dr. Xuan-Yu Wang has always been willing to assist me with any issues I faced. George Wright, Marc Pistilli and Raúl Loera Valencia have been a pleasure to work with. I would like to thank them for their company and their positive attitudes.

Finally, I would like to thank my family for their support and encouragement the past two years. They have supported me throughout my life, the good times and the hard times, and helped me mature into the person I am today.

LIST OF FIGURES

LIST OF ABBREVIATIONS

ANOVA – analysis of variance

BA – butyric acid

cGMP – cyclic guanosine monophosphate
CWT – continuous wavelet transformation

DA – decanoic acid

ENS – enteric nervous system

FFT – fast fourier transformation

HFLA – high frequency low amplitude

ICC – interstitial cell of Cajal
ICC-DMP – deep muscular plexus interstitial cells of Cajal
ICC-MP – myenteric plexus interstitial cells of Cajal
IJP – inhibitory junction potential
IP_3 – Inositol 1,4,5 trisphosphate

L-NNA – Nω-Nitro-L-Arginine
LFHA – low frequency high amplitude

MB – methylene blue
MCFA – medium chain fatty acid

NO – nitric oxide
nNOS – neuronal nitric oxide synthase

opm – oscillations per minute

PKG – protein kinase G

SCFA – small chain fatty acid
SEM – standard error of mean
sGC – soluble guanylyl cyclase
SP – substance P
SW – slow wave

W/W^v – WBB6F1/J-Kit^W/Kit^{W-v}/J (mutant)

TABLE OF CONTENTS

1. INTRODUCTION

1.1 Small intestine

The ultimate goal of motility patterns exhibited by the small intestine is to facilitate mixing and absorption of nutrients through optimal exposure to digestive enzymes. The two dominant motor patterns seen *in vivo* and *in vitro* are peristalsis and segmentation. Peristaltic movements propel luminal contents in an anterograde direction. Segmentation, originally observed by Cannon (1902), is depicted as stationary contractions dividing a string-like mass of content into many dividing bead like sections with barely any net content movement. The segmentation pattern aids in the digestion of food by mixing contents with gastric juices. Although these are described as two completely separate motor patterns, *in vivo* it is unlikely to observe the small intestine exhibiting only one at a time. Canon (1902) witnessed gradual propulsion of content associated with the segmentation motor pattern complex. The type of segmental contractions also depends on the physical properties of the food (Cannon 1902).

The gut wall is comprised of various layers including the mucosa, submucosa, muscularis, and serosa (Fig 1.1). Functionally as a whole, the layers act as a selective barrier to the external environment of the lumen, facilitate digestion, and propel digested content aborally (Stockinger et al., 2011). The muscularis comprises two smooth muscle layers, the longitudinal and circular smooth muscle. Separating these two muscle layers is

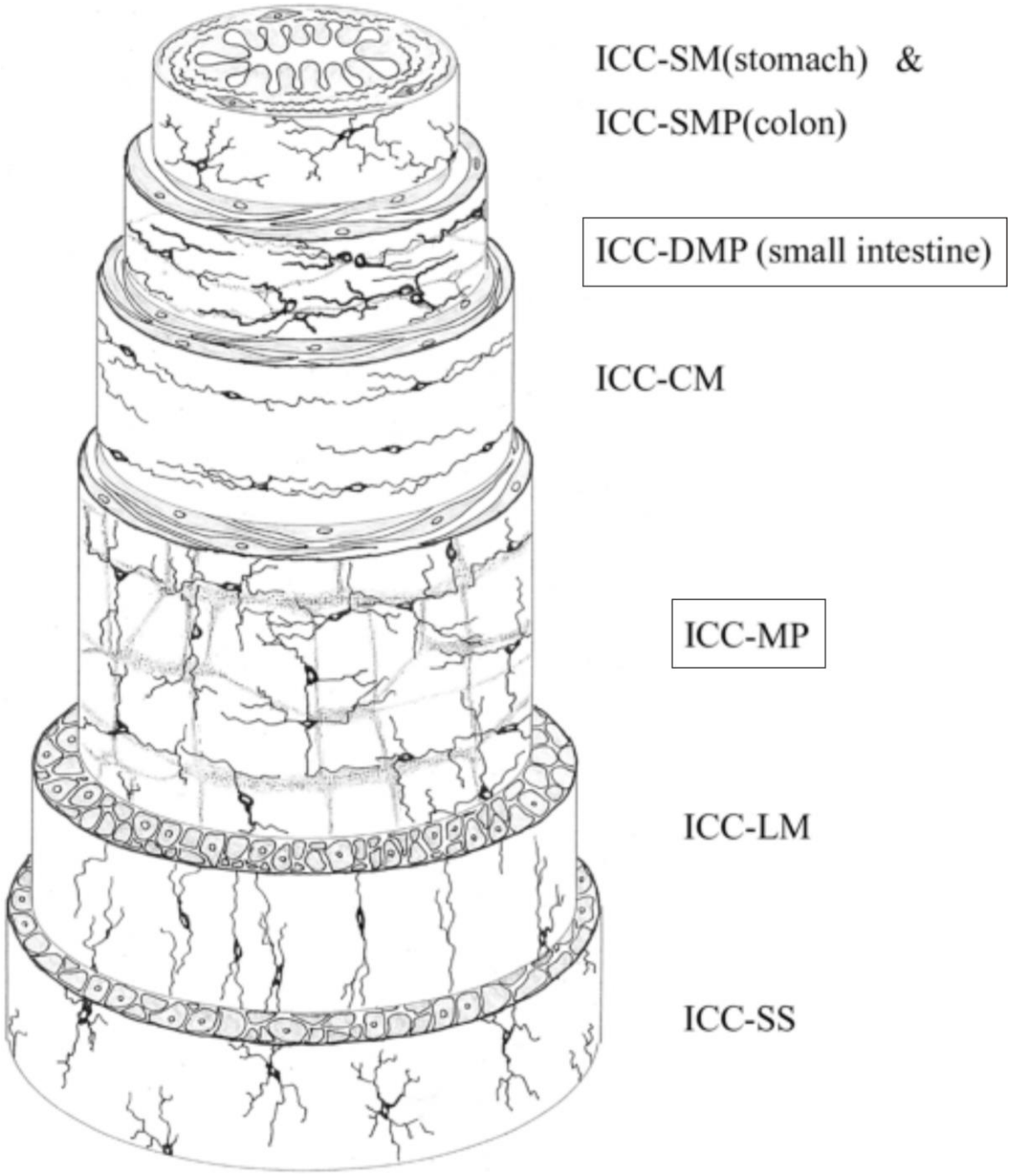

Figure 1.1 Residence of interstitial cells of Cajal in the small and large intestine. Beginning with the lumen (top) and ending with the serosa (bottom) the ICC networks of the small intestine [boxed] are present between the inner and outer division of the circular muscle, and within the myeneteric plexus separating the circular and longitiudinal muscle layers. Figure adapted from Komuro (2006).

a layer of connective tissue, within there, the myenteric plexus (Komuro, 2006). This plexus primarily contains neural bodies of the enteric nervous system (ENS) including intrinsic primary afferent neurons, as well as excitatory and inhibitory interneurons and motor neurons (Costa et al., 2000). Interstitial cells of Cajal (ICC) in this layer (ICC-MP) are responsible for generating pacemaker potentials which induce the rhythmic slow waves in the circular smooth muscle through electrical coupling. These slow waves play an important role in the pacing of motility patterns (Hudson et al., 2006, Der-Silaphet et al., 1998). In some vertebrate species, including humans and murine modes, the circular muscle can be differentiated into an inner and outer division; it is between these divisions the ICC of the deep muscular plexus (ICC-DMP) reside (Figure 1.1) (Olsson and Holmgren, 2001).

Ultimately, cellular communication is a necessity for individual cells to work in syncytium, allowing groups of cells to function as a tissue. This is especially true of the muscular layers in the intestine. It is hypothesized gap junctions allow cytoplasmic and electrical communication for reliable tissue coordination and function (Huizinga et al., 1992).

Smooth muscle cell contraction generates both segmentation and peristalsis motor patterns; however the mechanism of initiation and maintenance of said patterns are currently only speculated upon. Motor patterns in the small intestine are not reliant on central innervation (Schemann, 2005), thus it is likely the ENS and ICC populations communicate and influence muscle contractile activity.

Interstitial cells of Cajal

1.2.1 Interstitial cells of Cajal in the myenteric plexus

The ICC-MP morphology include triangular multipolar cells with three to five cytoplasmic processes projecting into the muscle layers and forming networks with adjacent ICC within the myenteric plexus (Komuro 2006, Garcia-Lopez et al., 2009). Structurally these energy demanding cells contain numerous mitochondria and caveolae (Garcia-Lopez et al., 2009).

ICC-MP networks are the electrical pacemakers responsible for the generation of the slow wave in smooth muscle (Fig 1.2) (Hudson et al., 2006, Der-Silaphet et al., 1998). These ICC facilitate communication, through gap junctions, to adjacent ICC and smooth muscle via active (regenerative) propagation (Liu and Huizinga, 1993). Slow waves observed in the musculature are rhythmic depolarizations in the membrane potential, likely initiated by intracellular calcium release (Hudson et al., 2006, Kito and Suzuki 2003, Lowie et al., 2011). In smooth muscle cells, slow wave associated intracellular calcium release is achieved by sarcoplasmic reticulum expulsion of calcium from intracellular stores via the inositol 1,4,5 trisphosphate (IP_3) IP3R-I pathway (Ward et al., 2003). However, calcium influx within a smooth muscle cell does not solely arise through the sarcoplasmic reticulum, but also from the extracellular ionic milieu. In ICC-MP, and likely smooth muscle cells, extracellular calcium enters through calcium channels: voltage-dependent calcium channels, the sodium calcium exchanger in reverse mode, and non-selective cation channels (Lowie et al., 2011).

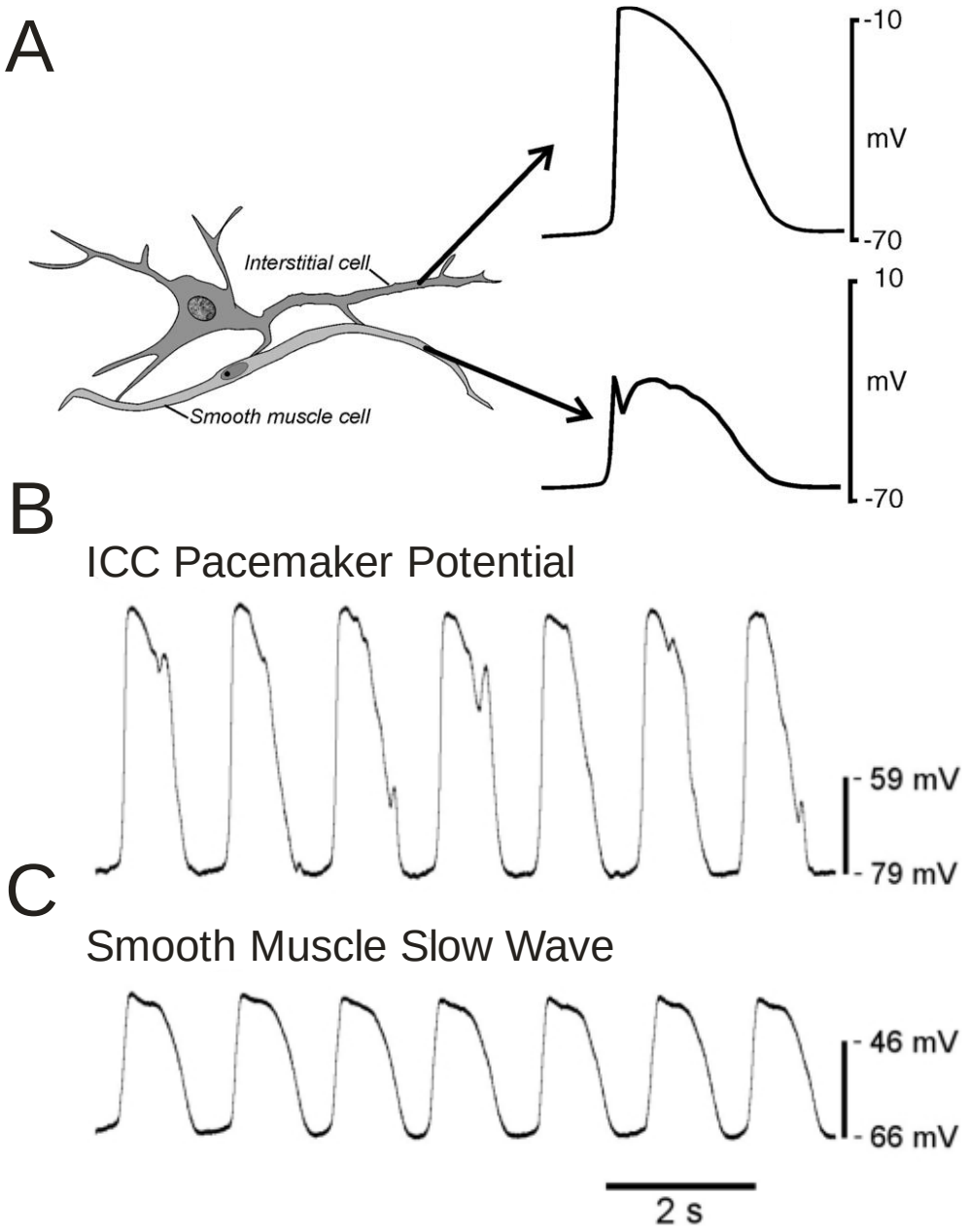

Figure 1.2 Schematic diagram and intracellular recordings of the electrical oscillatory activities generated from murine small intestine ICC-MP and smooth muscle cells. ICC-MP generate pacemaker potentials characterized by fast upstroke, large amplitude depolarizations (A, B). Slow waves generated in smooth muscle cells (A, C) display a different morphology including smaller amplitude depolarization and a repolarisation phase (A). Figure adapted from Kito et al. (2005; A), and Lees-Green et al. (2011; B, C).

These slow waves may be sufficient to reach a depolarization threshold and induce muscular contraction without the accompaniment of superimposed action potentials (Jimenez et al., 1996). While the previous statement is possible, generally excitatory influence on smooth muscle allows slow waves to reach a threshold for activation of L-type calcium channels, the onset of action potentials, and subsequently contractile activity of smooth muscle (Huizinga et al., 1997).

1.2.2 Interstitial cells of Cajal in the deep muscular plexus

The ICC of the deep muscular plexus are multipolar and form an uninterrupted network residing between the inner and outer circular muscle divisions. ICC-DMP cells are very closely associated with nerve bundles suggesting involvement in neural transmission to the muscle (Komuro 2006, Wang et al., 2003, 2005). In mice, the ICC-DMP of the small intestine share gap junctions with circular muscle cells and form close synaptic contacts with cholinergic, tachykinergic, and nitrergic nerves, indicating they may be under heavy neural control (Wang et al., 2003). These physical connections are supportive evidence for the hypothesis implicating ICC-DMP as neural mediators, a middleman between the ENS and smooth muscle. In addition to close physical proximity, ICC-DMP have also been shown to respond to both excitatory and inhibitory neurotransmission including acetylcholine, substance P, and nitric oxide (Garcia-Lopez et al., 2009). In an experiment by Wang et al., (2005), infection with *Trichinella spiralis* resulted in a parallel injury and recovery to both ICC-DMP and nerve varicosities. Injury was associated with loss of distension-induced burst like muscle activity (which may be

correlated to peristaltic movements). These results strongly support a secondary pacemaker role of the ICC-DMP reliant on the enteric nervous system. Currently, the specific role of ICC-DMP is still unknown due to lack of evidence; however many speculate they aid in pacemaker activity.

1.3 Neural Influence on ICC

1.3.1 Substance P and tachykinin receptors

There are three G-protein coupled tachykinin receptors (NK1r, NK2r and NK3r) which bind tachykinin neuropeptides with different affinities (Shimizu et al., 2008). Substance P (SP), the most represented excitatory tachykinin in the gastrointestinal tract has the highest affinity for NK1r, while neurokinin A and neurokinin B have highest affinity for NK2r and NK3r respectively (Faussone-Pellegrini 2006).

NKr immunoreactivity has been located on submucosal and myenteric neurons, as well as ICC-DMP populations and faintly present on ICC-MP networks (Faussone-Pellegrini, 2006). Through many immunohistochemical and fluorescent ligand-binding studies the specific tachykinin receptors have been localized to different cell types. NK1r and NK3r are present on enteric neurons, NK2r are dominant on smooth muscle and NK1r are expressed on ICC (Shimizu et al., 2008). Interestingly, NK1r was not localized to the smooth muscle layer, suggesting the excitatory effects of SP were mediated neurally and/or by ICC populations (Faussone-Pellegrini, 2006).

SP immunoreactive nerve fibers are more prominent in the deep muscular plexus than the myenteric plexus in all studied animal species; and in very close proximity to ICC-DMP (Faussone-Pellegrini, 2006, Shizimu et al., 2008). SP can diffuse easily in the intercellular space after synaptic release and reach the ICC-DMP not in direct contact with the nerve fiber (Faussone-Pellegrini, 2006).

Tachykinergic signalling via SP and NK1r is a finely regulated process. To prevent over stimulation by SP, neural signal cessation is achieved by either SP metabolism or tachykinin receptor internalization (Kirkwood et al., 2001). SP is a short polypeptide and can be easily metabolized by a variety of enzymes and peptidases, such as neural endopeptidase present in the gut (Kirkwood et al., 2001). The other postulated mechanism of SP signal termination involves the internalization of NK1r in the post-synaptic cell, where once internalized is protected from activation by extracellular agonists (Kirkwood et al., 2001, Grady et al., 1995). This likely happens in the ICC-DMP of the small intestine. NK1r – SP receptor ligand complexes internalized dissociate, the ligand is degraded and the receptor is either broken down as well or recycled back to the cell surface (Grady et al., 1995).

1.3.2 Nitric Oxide mediated relaxation

Nitric oxide (NO) mediates relaxation of smooth muscle via they action of cyclic guanosine monophosphate (cGMP) (Martinet al., 2005). When NO diffuses into a cell such as an ICC-DMP it binds with high affinity to the intracellular receptor nitric oxide-activated soluble guanylyl cyclase (sGC). Activation of this complex catalyzes the

production of cyclic GMP, a second messenger, which acts on ion channels via the activation of cGMP-dependent kinase, otherwise known as protein kinase G (PKG), to induce muscle relaxation in the rat small intestine (Huber et al., 1998). PKG can stimulate calcium activated potassium channels via phosphorylation of the channel or an associated regulatory protein (Robertson et al., 1993).

In the murine fundus, Groneberg et al. (2013) determined NO activated intracellular sGC in both smooth muscle cells and intramuscular ICC. The agonistic effect of NO binding to sGC in solely the ICC resulted in a relaxation of the muscle tissue. Therefore, NO mediated relaxation can occur via two cell type pathways: 1) by acting directly on the smooth muscle or 2) by acting on ICC.

In the mouse and rat nNOS is localized to neural bodies, including nerve fibers closely approaching ICC-DMP. ICC-DMP display high immunoreactivity to both sGC and PKG (Salmhofer et al., 2001, Ward et al., 2006). Thus, the ICC-DMP networks appear as prime targets for NO stimulus and may play a pivotal role in the relay of inhibitory neurotransmission from neural bodies to SMC.

1.4 Waxing waning phenomenon

Along the length of the intestine, the frequency of the slow wave decreases from the proximal to the distal end (Suzuki et al., 1986). In fact, it has been shown multiple times there is a 30% decrease in frequency from the duodenum to the ileum (Diamant and Bortoff, 1969). This suggests multiple pacemaker sites of step-wise decreasing frequency reside at various locations along the length of the small intestine.

On some occasions Hudson et al. (2006) noticed a rhythmic waxing and waning of the slow wave amplitude (Fig 1.3). This waxing waning phenomenon has been observed before by many investigators. One explanation provided by Diamant and Bortoff (1969) suggests in the areas between frequency plateaus, patterns of waxing waning appear due to competing signals from two dominant primary pacemakers. Evidence for the presence of two pacemakers has been shown before (Jimenez et al., 1996). Der-Silaphet et al. (1998) found this waxing waning pattern to persist in the presence of tetrodotoxin suggesting a myogenic origin of both pacemakers.

1.5 Luminal nutrients and small intestine motility

It is well known, unabsorbed luminal nutrients in the small intestine delay propagation and prolong the time content spends in contact with the villi of mucosal layer (Welch et al., 1988). In the human and rat models, ileal infusion of fatty acids significantly slowed the passage of content via a reduction in propulsive contractions within thirty minutes (Welch et al., 1988, Brown et al., 1990). At the time, the exact mechanism could not be determined, however a non-specific mechanism was speculated by Welch et al. (1988) hypothesising the lipid soluble compounds partition into cell membranes and interfere with cell coupling.

Infusion of the lumen with decanoic acid (DA), a medium chain fatty acid (MCFA), mimics luminal nutrients responsible for the initiating fed state and segmental motor patterns (Gwynne and Borstein 2007, Chambers et al., 2011). The segmental activity induced by DA and luminal nutrients in the intact small intestine was abolished

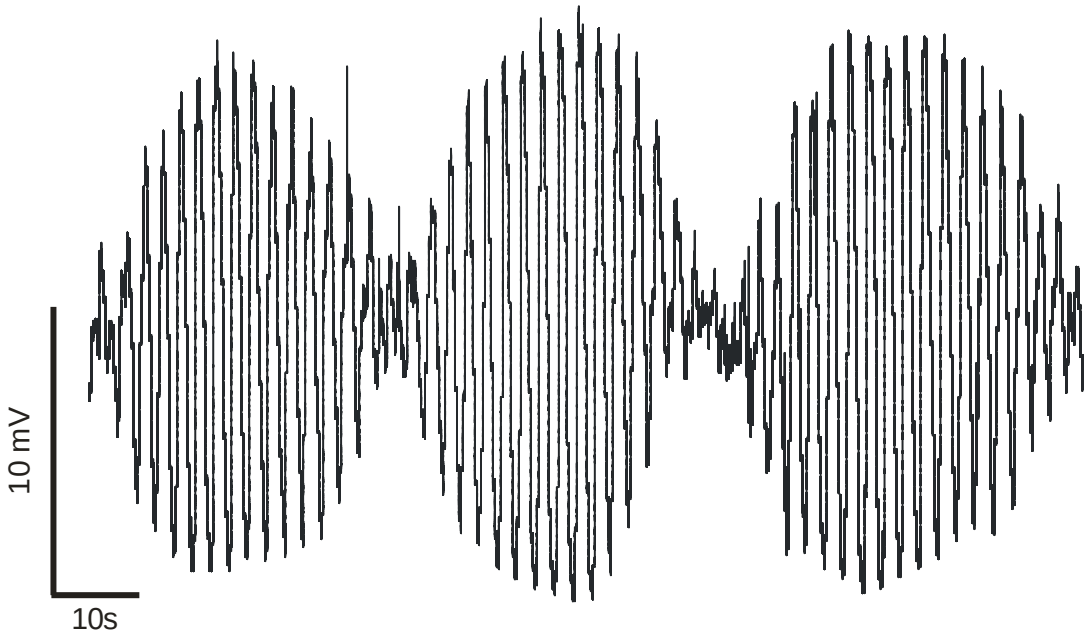

Figure 1.3 Waxing and waning of slow wave activity. Intracellular recording from a circular smooth muscle cell expressing the waxing waning phenomenon. The phenomenon is associated with rhythmic waning (decreases) in slow wave amplitude and depolarization.

with addition of TTX (Gwynne et al., 2004, Chambers et al., 2011) suggesting segmentation is a neurally controlled motor pattern; however the animal model used was the guinea pig. My results on the mouse model found DA could induce the waxing waning phenomenon. Thus there may be a link between waxing waning of the smooth muscle slow wave and the segmentation motor pattern.

1.6 Objectives

The aim of the work presented in this thesis was to understand the involvement and influence of both myogenic and neural control mechanisms and how together they contribute to the generation of the segmentation motor pattern. The main focus of this thesis was how the activity of circular smooth muscle correlated to functional motility studies in the mouse small intestine. I utilized intracellular electrical recording studies specifically to:

i. To determine the influence of intraluminal nutrients shown to induce segmentation on smooth muscle activity.

ii. To explore the role of myogenic pacemakers in the phenomenon of waxing and waning at the characteristic slow wave frequency seen from intracellular recordings of slow waves in the circular muscle of the murine small intestine.

iii. To determine the pacemaking capabilities of ICC-DMP and the influence of neurotransmitters on ICC-DMP activity.

1.7 Hypothesis

Generally, the hypothesis of this thesis suggests that initiation of the waxing waning phenomenon associated with segmentation activity requires the onset of a second pacemaker component in addition to the omnipresent ICC-MP slow wave activity. Specifics of the hypothesis are as follows:

Little is known about mechanisms involved in nutrient induced segmentation, however it is almost certain ICC play role in this pattern. This is because segmentation contractions are known to occur at the slow wave frequency in the mouse small intestine. Thus, addition of nutrients known to induce segmentation will likely affect the characteristic slow wave activity observed in the circular muscle layer.

Interactions of two or more pacemakers on opposite boundaries of the circular muscle thickness may interact through the small intestine musculature, as they do in the colon, to modify the existing ICC-MP driven slow wave to the waxing and waning phenomenon. The current roles of ICC-DMP in the small intestine are unknown. It is plausible ICC-DMP pacemaking activity when induced (via neurotransmission or other stimulants) interacts with the high frequency slow wave via coupling to produce a visible change in circular smooth muscle electrical activity.

.

2. METHODOLOGY

2.1 Animals

All research and handling of animals was approved by the Animal Research Ethics Board (AREB) at McMaster University in accordance with the standards set by the Canadian Council on Animal Care (CCAC). Female adult CD-1 mice (Charles River Laboratories International, Inc., Wilmington, MA) approximately 14 weeks of age were housed in the central animal facility of McMaster University under a 12 hour light, 12 hour dark cycle. Mice were housed in conventional cages with *ad libitum* access to both food and water. Female adult WBB6F1 J homozygous (wild-type) and WBB6F1/J-Kit^{W}/$Kit^{W\text{-}v}$/J (W/W^{v} mutant, W^{v}) c-Kit knockout mice (The Jackson Laboratory, Bar Harbor, Maine) aged approximately 8 weeks were kept in a clean room with the same caging conditions as CD-1 mice.

Mice were euthanized by cervical dislocation. Immediately after cervical dislocation, the abdominal cavity was opened and the small and large intestine, from proximal duodenum to distal colon, was carefully dissected out. The excised intestines were placed into fresh Krebs' solution. Krebs' solution is a buffered isotonic solution which mimics the bodily fluids of an animal; and keeps tissue alive after excision.

2.2 Tissue Preparation

Small segments of the jejunum (1-2 cm) were prepared for intracellular recording. The mesenteric fat was carefully cut off with fine point scissors and subsequently opened

along the length of the mesenteric border and pinned flat on a Sylgard gel dish, mucosa facing upwards. Tissue was continuously submerged in oxygenated Krebs' solution and maintained at room temperature until experimentation; then the solution temperature was increased to 37^{o}C and the tissue was allowed to equilibrate for the duration of one hour. The Krebs' solution was buffered with HCl_{aq} to maintain a pH range from 7.3-7.4. In order to abolish contractile activity of the smooth muscle to enable cellular impalements, 0.5 µM of nicardipine was added to the Krebs' solution unless otherwise stated.

2.2.1 Circular muscle preparation

Segments of the jejunum approximately 1 cm in length were used for standard circular muscle preparations. After the tissue was opened along the mesenteric border and pinned down flat the luminal contents were removed via washes with Krebs' solution. Once clean, the mucosal and submucosal layers were carefully peeled off using fine dissection forceps to expose the circular smooth muscle layer.

2.2.2 Hemi dissection partitioned chamber preparation

A hemi-dissection preparation was utilized in order to determine how reagents added to the mucosa influenced circular muscle electrical activity. The microelectrode required for intracellular recordings cannot penetrate the mucosa and submucosa layers, so a hemi-dissection was necessary to record from the circular muscle in control conditions while stimulus was perfused onto the mucosa intact half. For this experimental setup a more complex Sylgard gel dish was designed. The dish was separated into two halves by a plastic comb (partition) with a single 1 cm wide gap at the

center to allow the tissue sample to be pinned (Fig 2.1). In this case 2 cm segments of the jejunum were centered in the dish. The mucosa and submucosa was left intact on half the preparation and excised on the other half, the cut off being the division where the comb inserts. The seal was tested by the use of colored dye.

2.2.3 Small preparation

To paralyze tissue and prevent muscle contraction without the use of an L-type calcium channel blocker (nicardipine), small preparations were designed. Tissue was prepared as explained in section *2.2.1*. After the mucosa and submucosa layers were peeled off, leaving a 1 by 1 cm (approximately) preparation, multiple smaller 2 by 2 mm squares were pinned within. The surrounding circular muscle of the initial preparation was then excised from the tissue sample. This left multiple isolated small non-contracting circular muscle preparations to record from.

2.3 Intracellular recording technique

Intracellular recording is a powerful technique to observe the electrical activity of a single cell. This method is capable of recording voltage changes in the membrane potential. It is commonly used to study how cells respond to stimulus via the opening of ion channels.

2.3.1 Electrophysiology

Electrical activity from individual circular smooth muscle cells were recorded by impalement with borosilicate glass micropipettes (fire polished; length: 7 cm; O.D: 1.5

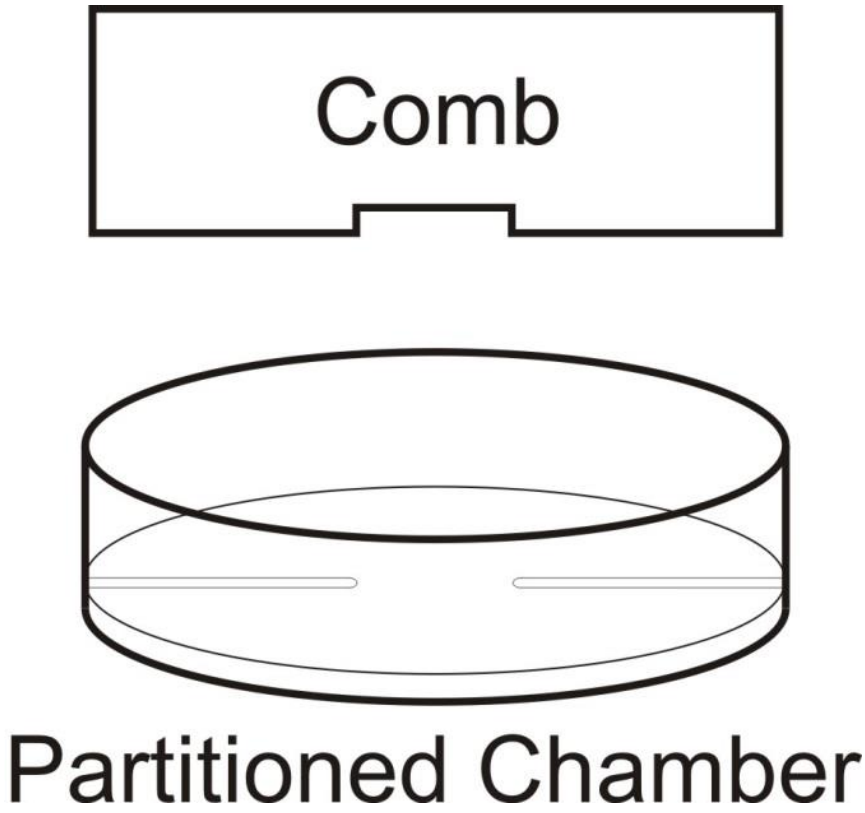

Figure 2.1 Diagram of the partitioned chamber. The Sylgard gel was formed to allow the insertion of a plastic partition (comb) to separate the dish into two halves, allowing the perfusion of different solutions onto either half without leakage.

mm, I.D: 0.86 mm) filled with 3 M KCl and fabricated to yield resistance between 30-70 MΩ. Use of MultiClamp 700B amplifier (Axon Instruments, Molecular Devices, Sunnyvale, CA, USA) recorded electrical signals from smooth muscle. These signals were digitized at an acquisition rate of 2 kHz using a Digidata 1322A acquisition system (Axon Instruments). Direct current was used with zero intensity to record membrane potentials of circular smooth muscle cells near the level of the deep muscular plexus.

2.4 Solutions, drugs and reagents

Tissue preparations were kept in oxygenated (95% O2, 5% CO2) Krebs' solution (118.1 mM NaCl, 1.0 mM NaH_2PO_4, 1.2 mM $MgSO_4$, 2.5 mM $CaCl_2$, 4.8 mM KCl, 11.1 mM glucose, 25 mM $NaHCO_3$). All salts were of high purity purchased from local sources. All drugs and reagents were dissolved in deionized water except for decanoic acid (DA) in dimethyl sulfoxide (DMSO), Nω-Nitro-L-Arginine (L-NNA) in 50 mM HCl_{aq}, and nicardipine in 50% ethanol. DMSO never exceeded 0.1% total volume during experimentation. Drugs were dissolved daily as required except nicardipine (stored at -20^{o}C) and tetrodotoxin (TTX; stored at -20^{o}C).

2.5 Data analysis and statistics

Raw data from current clamp voltage recordings were extracted from Clampex using a personal computer. Slow wave frequency, amplitude, and duration parameters were calculated from voltage time recordings (see *3.2.3*).

For continuous wavelet transformation (CWT) analysis, approximately four minutes per sample of continuous uninterrupted current clamp voltage recordings were

reduced to a sampling rate of 200 kHz and imported into Matlab (MathWorks, Natick, MA, USA). The voltage time parameters were then analyzed by the software to produce an end product including frequency power spectrum, and a two-dimensional frequency over time contour map.

All data are presented as mean ± standard error of mean (SEM) of n experiments, where n is a value from a different animal. Data means were compared using paired Student's t-test and/or one way analysis of variance (ANOVA) employing a Bonferroni correction, where appropriate.

3. LUMINAL NUTRIENTS AND PACEMAKER POPULATIONS

3.1 Introduction

After a nutritious meal the predominant motor pattern exhibited by the small intestine is the segmentation motor pattern. This phenomenon consists of stationary circular muscle contractions which divide segments of the small intestine into isolated bead-like compartments where content is exposed to gastric juices and the villi for optimal absorption (Canon, 1902). Early studies by Welch et al. (1988), and Brown et al. (1990) on human and rat models determined infusion of fatty acids reduced peristalsis movements and promoted a "fed state" of segmental behavior; however a specific mechanism could not be speculated at the time.

Common debate arises over the neurogenic or myogenic origin of the segmentation motor pattern, with strong arguments for each over many animal models. Gwynne et al. (2004) experimented on the luminal effects of DA in the guinea pig small intestine, and found DA could induce multiple types of TTX sensitive segmental contractions as observed by spatio-temporal mapping. This pattern could be abolished by addition of TTX or muscarinic blockade indicating excitatory neurotransmission was required for the onset of DA induced segmentation. Additional inquiries into nutrient induced segmentation in the guinea pig determined amino acids, L-phenylalanine and L-tryptophan, were capable of generating stationary contractions (Gwynne and Bornstein, 2007). The guinea pig model has weak slow wave pacemaker activity, and thus the ICC populations' involvement was dismissed with reasonable evidence. However, there was

remarkable rhythmicity and slow wave like appearance in the extracellular recordings of the large excitatory junction potential and single action potential associated with stationary contractions.

Mouse and rat murine models express easily distinguishable pacemaking activity in the form of slow waves. Slow waves play a more prominent role in motility patterns in these animal models than in the guinea pig where pacemaker activity is stimulated, not omnipresent, and neurally mediated action is much more visible (Donnelly et al., 2001). In the mouse, segmentation activity occurs at the pacemaker frequency of ICC-MP (Thuneberg and Peters, 2001). Additionally, an *in vivo* study of rat small intestine activity obtained via MRI data acquisition of whole jejunum found peristalsis and segmentation occurred at ~ 0.45 Hz, the slow wave frequency (Ailiani et al., 2009). Fast fourier transformation (FFT) analysis of peristalsis revealed one dominant high frequency while segmentation revealed two dominant high frequency components (Fig 3.1). In both cases the low frequency components found were dismissed as artefacts of slow changes in the position of the GI tract.

Indeed these FFT results are very similar to those obtained by Suzuki et al. (1986) in their investigation of the waxing waning phenomenon of slow waves in the circular muscle (Fig 3.1). In control conditions a steady non fluctuating slow wave can be observed from intracellular electrode recordings of exposed circular smooth muscle. However, in some scenarios waxing and waning of the slow wave amplitude can be observed spontaneously. Bortoff (1965) originally presented the hypothesis suggesting

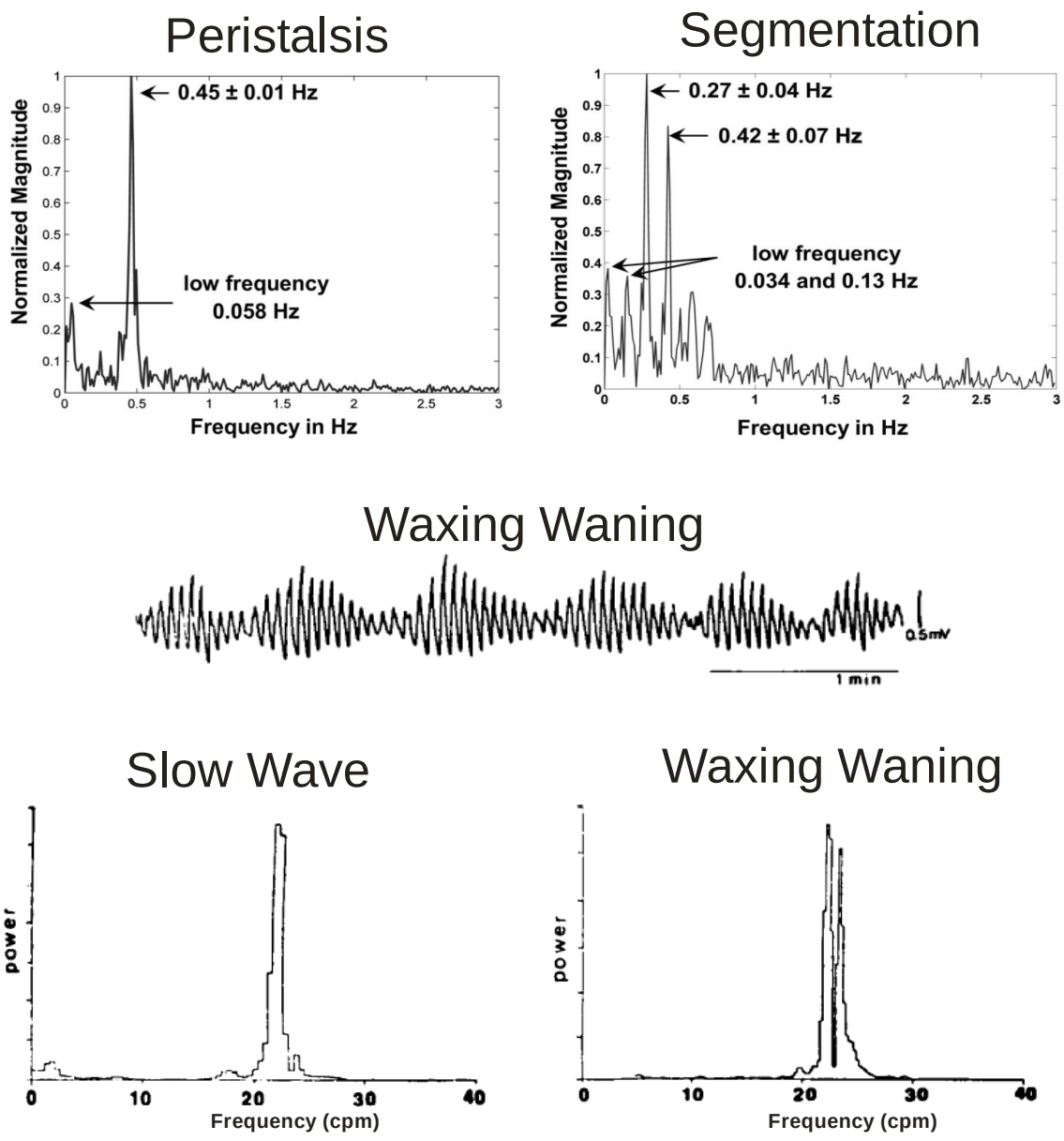

Figure 3.1 Comparisons between motor patterns and cellular electrical activity. FFT analysis of an *in vivo* MRI during peristalsis and segmentation compared to a slow wave and the waxing waning phenomenon. The slow wave and peristalsis both involve one dominant frequency component while multiple oscillators are involved in segmentation and waxing waning. Figure adapted from Suzuki et al., (1986) and Ailiani et al., (2009)

waxing waning result from the interaction of two pacemakers of slightly different frequencies. The work by Suzuki et al. (1986) later strengthened this hypothesis with supporting data from FFT analysis of the waxing waning phenomenon. Compared to the non-fluctuating slow wave, which contained one dominant frequency after FFT analysis, waxing waning consistently presented two peaks at slightly different frequencies. However, there are some flaws in this theory. Firstly, the only cells capable of rhythmically oscillating at the frequencies presented in the FFT are the ICC-MP (Der-Silaphet et al., 1998). In the scenario suggested by Suzuki et al. (1986), in addition to the present dominant pacemaker, another must spontaneously arise. Since ICC-MP networks spread electrical signals actively (Liu and Huizinga, 1993) these two competing pacemakers would then interact within in the same plane and either annihilate or summate. While summation of two sinusoidal waves at slightly different frequencies traveling in opposing directions does produce a waxing waning pattern, the amplitudes are also summated which is not the case in tissue experiments; the amplitude remains the same. Secondly, FFT assumes the signal analyzed is stationary; the algorithms provide power density spectrum information of only the frequency domain, thus all time domain information is lost. Time-frequency algorithms such as the wavelet transformation are a better approach in determining the frequency of the time-varying signals in biological systems (Beck et al., 2006). The double peak result from FFT analysis could be an artifact picked up by a variation in time of the high frequency component. Thus, wavelet analysis of the data should be performed to isolate variable frequency components and shed light on any additional oscillators involved in production of the waxing waning phenomenon.

Disregarding the flaws of the FFT, in Figure 3.1 there is a strong correlation between the single peak of whole organ peristalsis and smooth muscle cell slow waves, and between the multiple peaks of segmentation and waxing waning. It seemed logical to investigate the effects of luminal nutrients shown to induce segmentation while recording from a single cell.

Gwynne and Bornstein (2007) found that DA as well as the amino acids L-phenylalanine and L-tryptophan, could induce segmentation in a quiescent guinea pig small intestine. Since DA is a medium chain fatty acid, it would also be of interest to see how a short chain fatty acid (SCFA) such as butyric acid, a common metabolic product of anaerobic bacterial fermentation, would influence the electrical pattern. SCFAs can reach luminal concentrations of 20 mM in the distal small intestine (Diener et al., 1996, Macfarlane and Macfarlane, 2012).

Generally, to record from the circular muscle the mucosa and submucosa are peeled away so the micro electrode can safely penetrate the exposed smooth muscle cells. However this setup does not reveal how nutrients influence smooth muscle electrical patterns at the level of the mucosa. These nutrients are present in the lumen *in vivo* and come in contact with the villi, thus they likely induce a response at the level of the mucosa. In addition to the exposed circular muscle preparations, a partitioned chamber (Fig 2.1), similar to that used by Bayguinov et al. (2007), was designed to separate a hemi-dissected tissue preparation and record the effects on nutrients on the mucosa from the circular muscle.

3.2 Methods

Intestinal jejunum segments from adult female CD-1 mice were used for all intracellular recording experiments. Information regarding animal handling and intestinal excision can be found in section 2.1 and 2.2 respectively.

3.2.1 Circular muscle experiments proper

Tissue preparations were continuously perfused (4 mL min^{-1}) with oxygenated Krebs' solution at 37^{o}C viewed under a high powered inverted microscope (Zeiss Axiovert S100 TV). Outflow (16 mL min^{-1}) was discarded into a waste container. After the tissue sample was equilibrated at 37^{o}C for one hour experimentation could begin. The recording microelectrode was carefully lowered to just above the surface of the tissue and penetrated individual cells within the circular muscle layer with the aid of a micro manipulator (Axon Instruments). Once a disturbance in the voltage recording was detected, attempts to buzz in the electrode (50 ms pulse) into a smooth muscle cell commenced. Generally, observation of a slow wave determined if the insertion was successful.

In all preparations, controls were obtained by recording uninterrupted electrical activity for a period of at least five minutes from a single circular smooth muscle cell. After the five minute control recording, nutrient reagents (1 mM DA, 10 mM BA, or a mixture of 5 mM L-tryptophan and 5 mM L-phenylalanine) were then added to the inflow reservoir of fresh Krebs' solution and subsequently perfused onto the tissue samples. To observe the change in pattern induced by the DA without neural input, 0.5 µM TTX was

added 10 minutes prior to recording. After a continuous 5 minute control recording tissue preparations were challenged with 1 mM DA. In tissue samples where the entire control recording consist of the waxing waning phenomenon (un-stimulated), pharmacological agents used to assess the pattern were, 1 µM atropine, or 0.5 µM TTX. All drugs were added to the inflow reservoir and subsequently perfused with fresh Krebs'.

3.2.2 Hemi-dissection experiments proper

The hemi-dissected tissue sample was allowed to equilibrate at 37^{o}C one hour prior to experimentation. The barrier (comb) was inserted before the warmed Krebs' solution was perfused onto the tissue sample. Once inserted, the barrier separated the mucosa intact and exposed circular muscle halves. Each side was perfused (4 mL min^{-1}) by a separate inflow reservoirs. Microelectrode insertion into the exposed circular muscle half was as described previously (See *3.2.1*). During experimentation the microelectrode penetrated the exposed circular muscle layer as close to the barrier as possible.

Controls were obtained by recording uninterrupted electrical activity for five minutes. After the control period, fatty acids (1 mM DA, 10 mM BA) were added to the inflow reservoir of Krebs' solution of the mucosa intact side. When tissue did not respond to fatty acid perfusion after a period of 40 minutes, as determined by real-time visual observation of electrical activity, the nutrient containing Krebs' solution was then perfused onto the control half (exposed circular muscle) of the preparation.

3.2.3 Data analysis

Raw data of slow wave electrical activity was recorded and extracted using Clampex 9.2 software (Molecular Devices), and analyzed to determine the frequency, amplitude and duration parameters. Microsoft Excel (Redmond, WA) was used for subsequent data transformations and calculations. The parameters of the slow wave (SW) were calculated as follows:

Frequency of SW = Number of SW / t (Fig 3.2)

where SW is a single depolarization and repolarization; t is time in minutes

Duration of SW = $t_{1SW} - t_{0SW}$ (Fig 3.2)

where t_{0SW} is the time in seconds at the beginning of a slow wave; t_{1SW} is the time at the end of a slow wave

Amplitude of SW = $maxA_{SW}$ – baseline (Fig 3.2)

where $maxA_{SW}$ is the maximum amplitude of the slow wave; baseline is the lowest amplitude prior to a slow wave.

For CWT analysis, approximately four minutes per sample of continuous uninterrupted current clamp voltage recordings were reduced to a sampling rate of 200 Hz and imported into Matlab (MathWorks). The voltage time parameters were then analyzed by the software to produce an end product frequency power spectrum, and a two-dimensional frequency over time contour map.

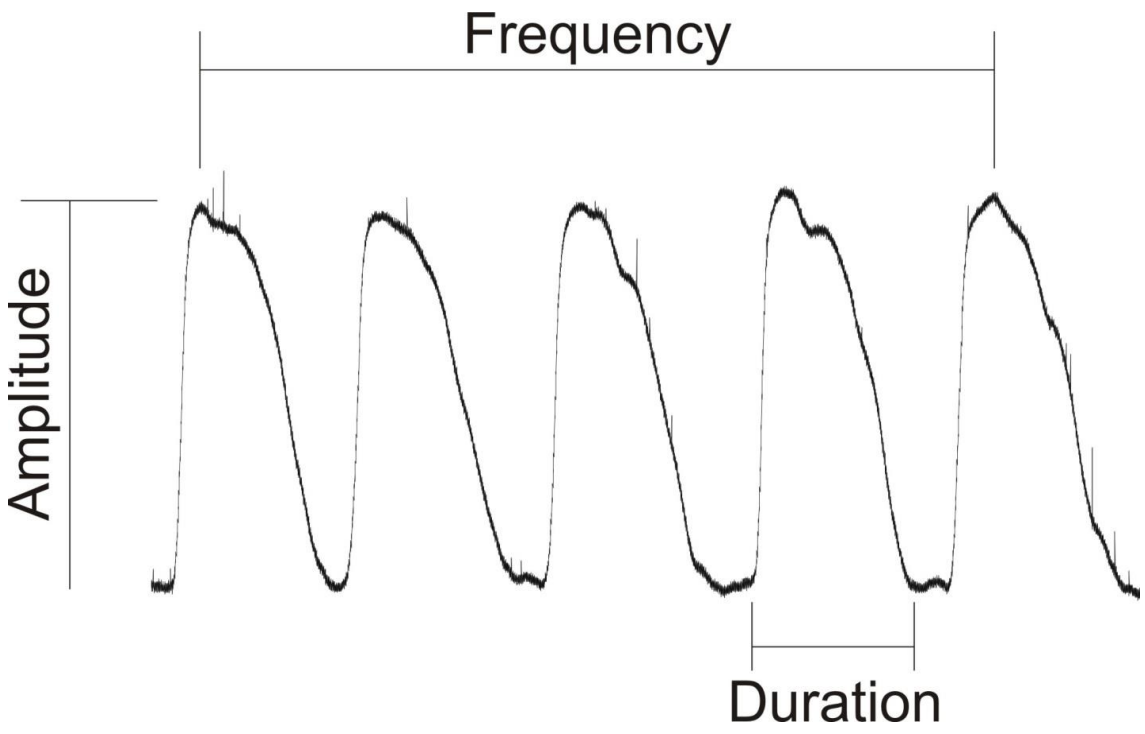

Fig 3.2 Analysis of intracellular current clamp recording experiments. Acquisition of frequency, amplitude, and duration parameters of electrical slow wave oscillations were measured over time. The same parameters are recorded before and after the addition of compounds.

3.3 Results

3.3.1 Circular muscle preparation

In circular muscle preparations perfusion of 1 mM DA induced a rhythmical waxing waning electrical pattern from a steady, non-fluctuating slow wave (n=8, Fig. 3.3 A, B). The time it took to establish this wave pattern varied among preparations (n=8, mean 8.44 ± 1.46 min). Waxing and waning gradually returned to the original slow wave pattern with a washout of fresh Krebs' solution (n=7, Fig. 3.3 C). In the present study, waxing and waning is characterized by a 50% decrease in waning (minimum) compared to waxing (maximum) amplitude, and a depolarization of resting membrane potential associated with waning (Fig 3.4), as initially reported by (Suzuki et al., 1986).

DA was dissolved in DMSO. A necessary control was to determine if addition of DMSO vehicle itself was responsible for the waxing waning phenomenon. In control experiments, addition of DMSO vector (1/1000 dilution) did not alter slow wave parameters or induce waxing waning (n=3).

In some recordings the waxing waning pattern was present initially with no external stimulation. To determine if sustenance of the waxing waning pattern was reliant on the ENS, neural antagonists were perfused to tissue. Neither 1 µM atropine (n=7) nor 0.5 µM TTX (n=2) were able to abolish the waxing phenomenon.

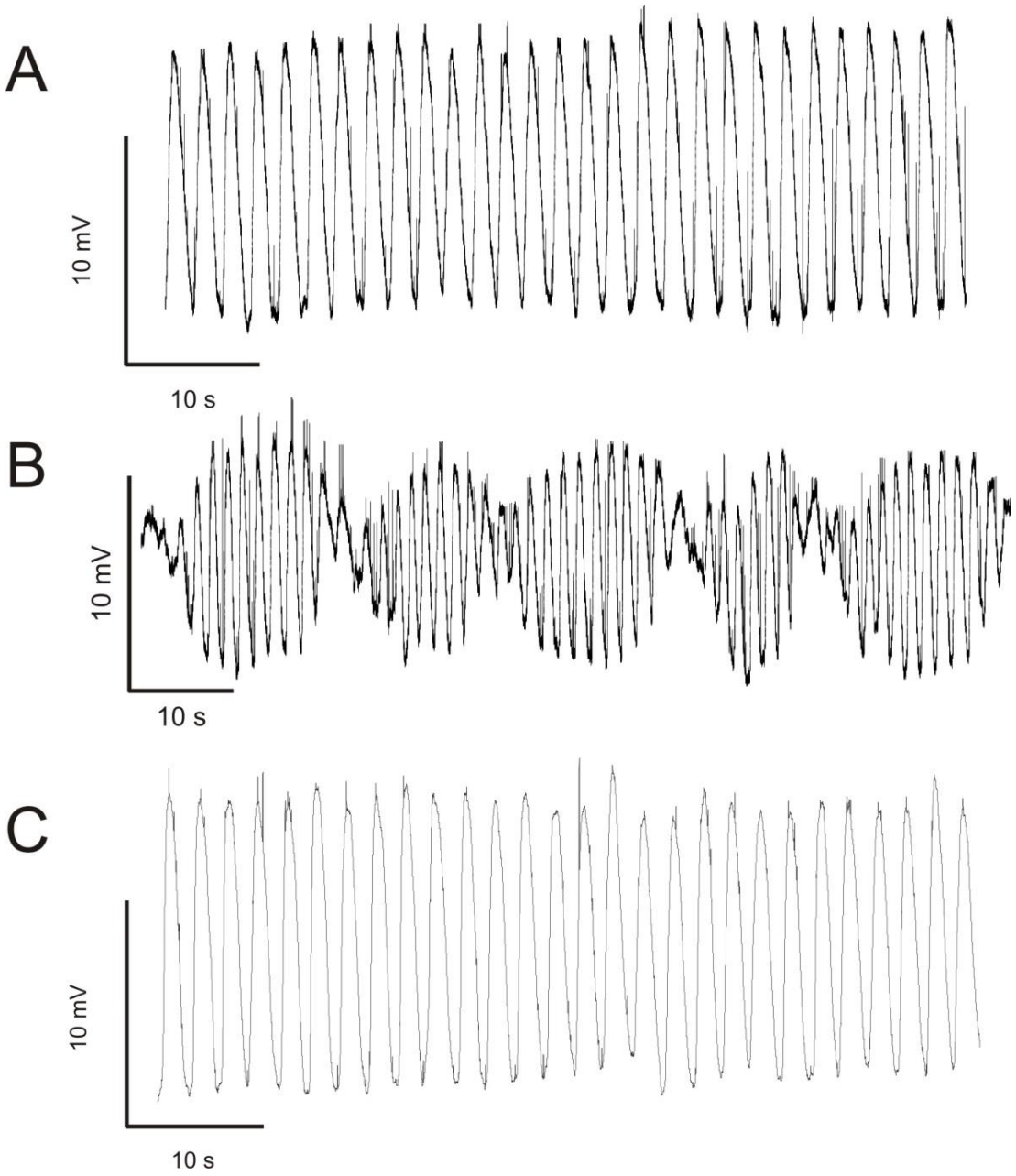

Figure 3.3 Intracellular recording of DA perfusion on circular smooth muscle. Circular muscle cell exhibiting a steady slow wave (A). After the addition of 1 mM DA a waxing waning pattern emerged (B). The waxing waning pattern was abolished by washout, restoring the original slow wave pattern (C).

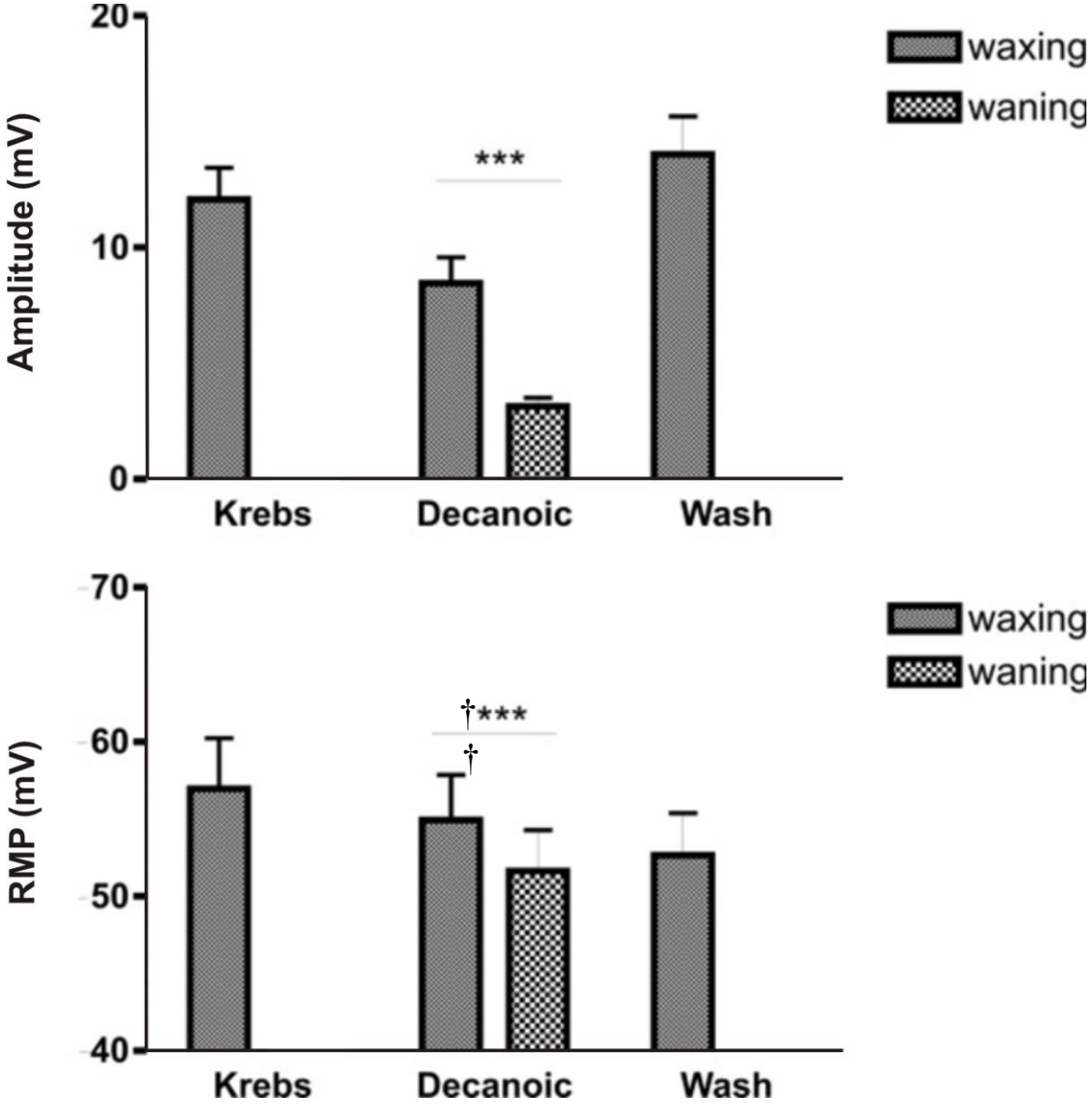

Figure 3.4 Statistical analysis of the waxing waning phenomenon. The waning (minimum) amplitude is significantly smaller than the waxing (maximum) amplitude (<50 % waxing amplitude), and associated with a depolarization of the resting membrane potential. (mean ± SEM; n=8 Krebs', Decanoic; n=7 Wash; ***p<0.001, Amplitude of Decanoic waxing vs. Decanoic waning; †***p<0.001, RMP of Decanoic waxing vs Decanoic waning)

While the ENS is not necessarily required to maintain the phenomenon it may be required in the initiation of waxing waning. 1 mM DA was perfused onto the tissue in the presence of 0.5 µM TTX. TTX had no effect as DA was still able to induce the waxing waning oscillatory pattern in the presence of neural blockade (n=5, Fig 3.5). Figure 3.6 shows the statistical analysis of change in slow wave parameters during the waxing waning phenomenon.

Similar to the hypothesis of Bortoff (1965) and Suzuki et al. (1986) based on their FFT analysis of waxing waning, it is likely the waxing waning phenomenon is induced by the onset of another electrical oscillator capable of interacting with the original dominant high frequency oscillator (the ICC-MP network) through the circular muscle layer. CWT analysis of the data was performed as opposed to FFT analysis in order to isolate frequency components of a time varying signal, and shed light on any additional oscillators involved in producing the waxing waning phenomenon. CWT analysis of a control slow wave (Fig 3.7A) reveals only one dominant high frequency component (Fig 3.7B). The time-frequency contour plot of mean power, which provides more insight on the presence and variation of frequency components over time, demonstrates only one oscillator is present during regular slow wave activity (Fig 3.7C). The waxing waning phenomenon on the other hand (Fig 3.8A), revealed a distinct low and high frequency component (Fig 3.8B). This is supported by the time-frequency contour plot of mean power (Fig 3.8C) which clearly depicts simultaneous activity of the high and low frequency components.

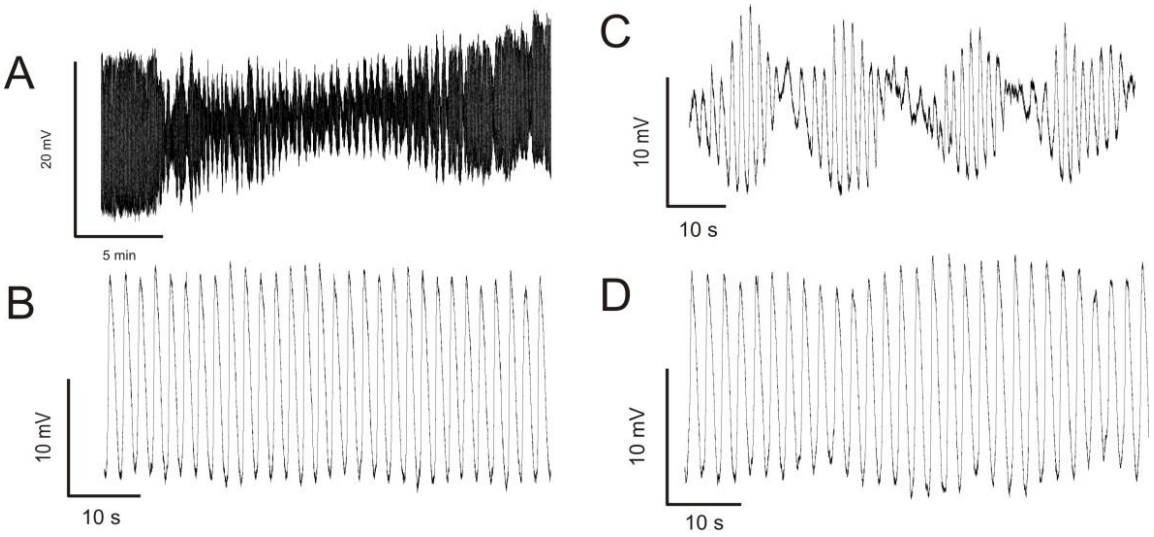

Figure 3.5 Intracellular recording of circular muscle in the presence of neural blockade. Control slow wave in presence of 0.5 µM TTX challenged with 1 mM DA induces waxing waning pattern which fades away with washout of fresh Krebs' without TTX (A). Isolated components from the same recording shown in a smaller time frame: slow wave (B), induced waxing waning (C), and restoration of the slow wave (D).

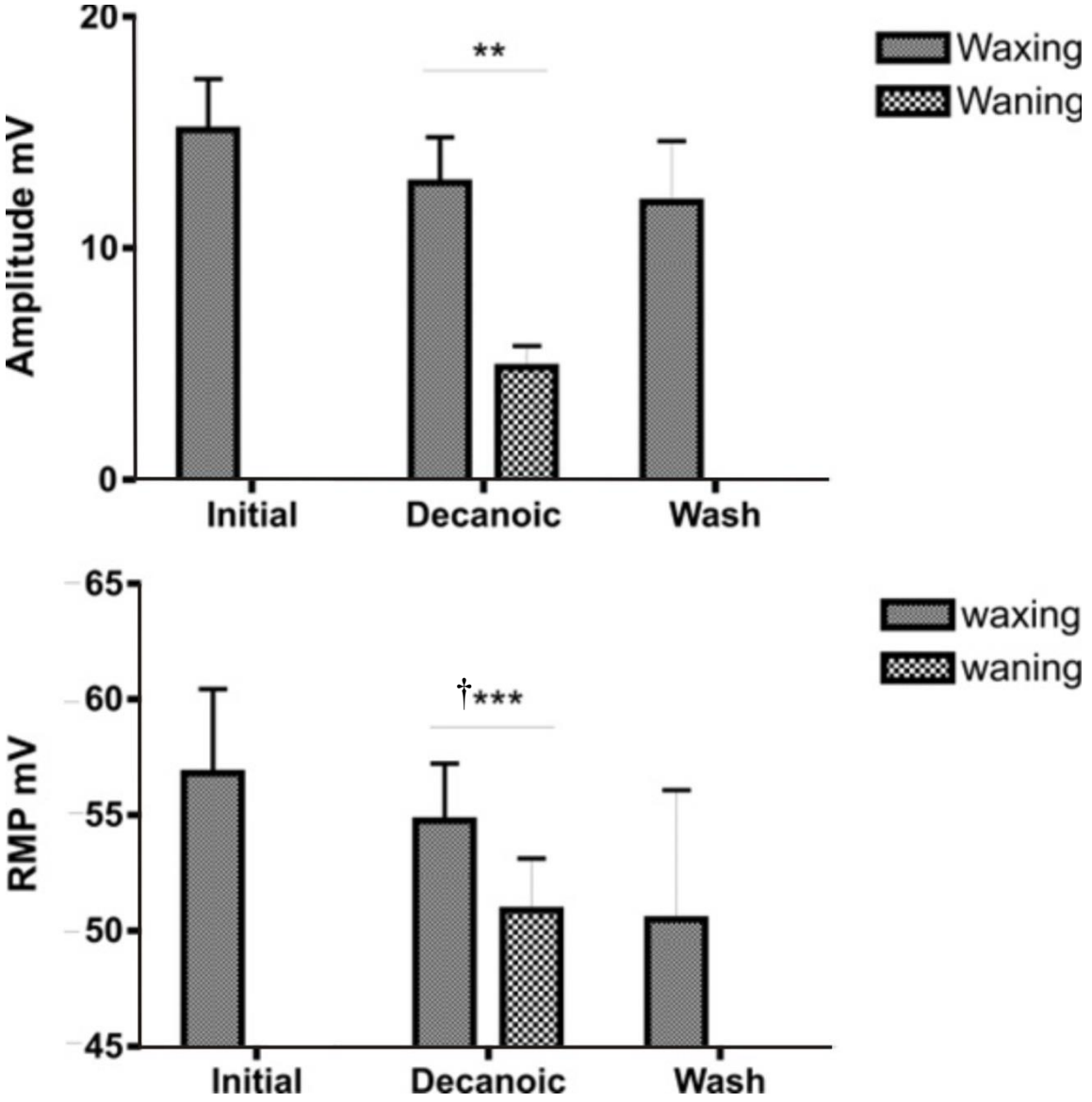

Figure 3.6 Statistical analysis the waxing waning phenomenon in neural blockade. In the presence of 0.5 µM TTX the waning (minimum) amplitude is significantly smaller than the waxing (maximum) amplitude (<50 % waxing amplitude), and associated with a depolarization of the resting membrane potential. (mean ± SEM; n=5 Initial, Decanoic; n=2 Wash; **p<0.01, Amplitude of Decanoic waxing vs. Decanoic waning; †***p<0.001, RMP of Decanoic waxing vs Decanoic waning)

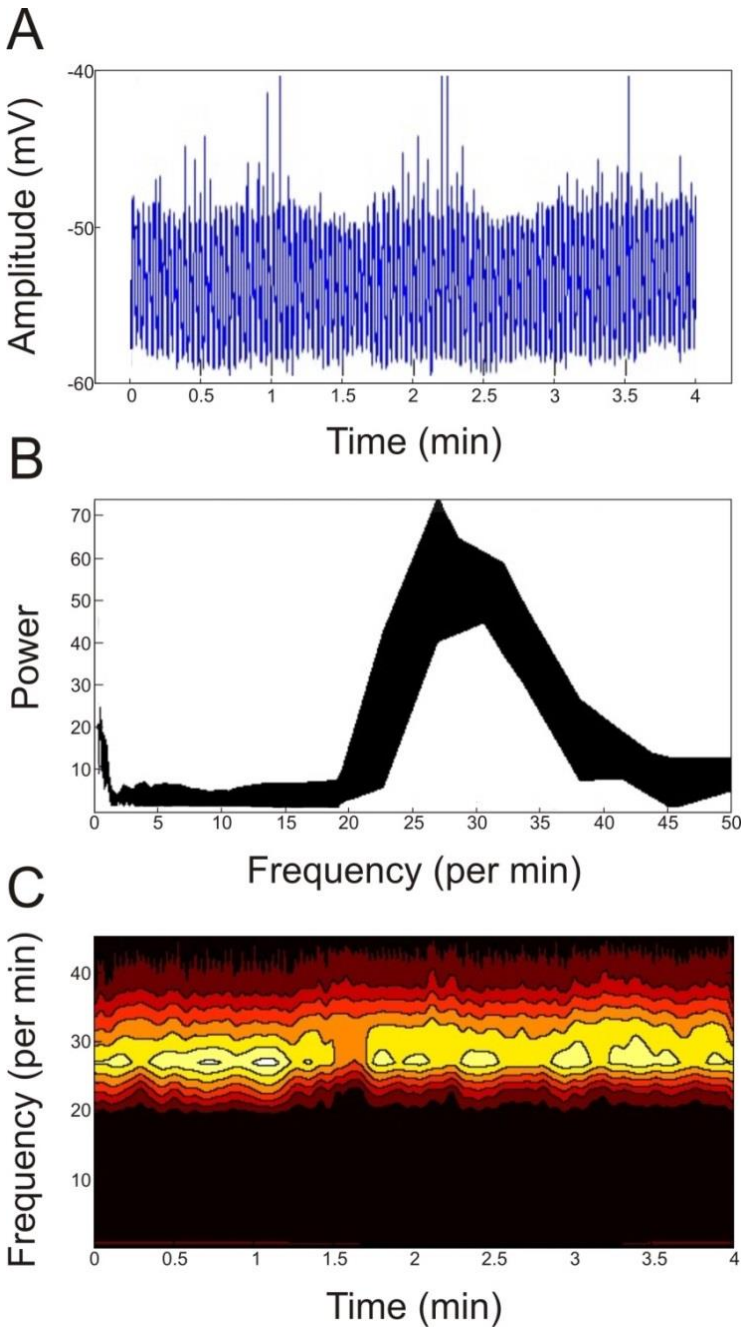

Figure 3.7 Frequency components in a standard slow wave. Intracellular electrical activity of circular muscle in control conditions (A). Continuous wavelet transformation analysis shows frequency distribution of source (B). Time-frequency contour plot of mean power (continuous wavelet transform analysis) shows a high frequency component (C).

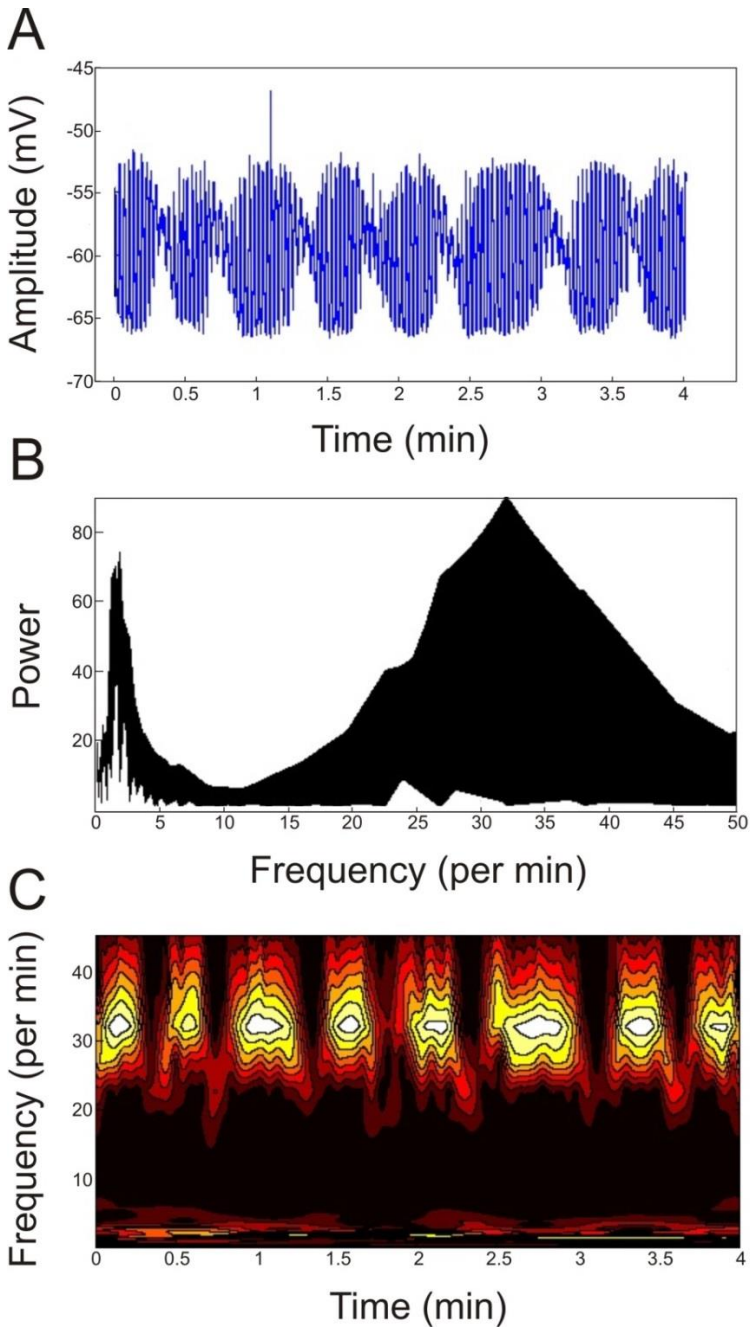

Figure 3.8 Frequency components in the waxing waning phenomenon. Intracellular electrical activity of circular muscle in the presence of 1 mM DA (A). Continuous wavelet transformation analysis shows frequency distribution of source (B). Time-frequency contour plot of mean power depicts the presence of both high and low frequency components (C).

This data suggests the waxing waning phenomenon is induced by the onset a low frequency component.

Samples analyzed by CWT of the standard, non-fluctuating slow wave (Table 3.1), all expressed a high frequency component (n=21), similar to Figure 3.7. Unexpectedly, in some of the control samples (9 of 21) a low frequency component could be isolated. On second thought, this is not surprising; the waxing waning pattern can emerge and resolve itself from a characteristic slow wave without external stimulus, and thus it should be expected to sometimes find a low frequency component. Additionally, it is important to note the low frequency component may always be present but weak; it may be masked due to the dominating power of high frequency component. When the low frequency component is visible in the power frequency spectrum of a control slow wave, it is generally much weaker in power than the high frequency component. It became necessary to quantify this by determining the power ratio between the high frequency (HF) and the low frequency (LF) component. Generally, if the HF:LF ratio is greater than 3.0 the low frequency component does not appear on the CWT contour map (frequency over time). On the other hand, a HF:LF ratio less than 3.0 can be picked up on the contour map. It should be mentioned the 3.0 ratio cut-off is arbitrary. Investigation into the effectiveness of the cut-off found given solely the HF:LF ratio, the influence on the slow wave pattern could be predicted with 86% accuracy (n=27).

The waxing and waning pattern consistently depicted a high frequency and a low frequency component (n=12, mean 2.6 ± 0.15 opm). It should be mentioned some of the data samples (7 of 12) on the waxing waning phenomenon contributed to the sample size

Table 3.1 Analysis of Frequency Components in Different Experiments

Experiment stage	N	# Frequency Components	LF (mean)	N(exp)	HF (mean)	N(exp)	HF:LF ratio
Control	21	1.4 ± 0.11	3.8 ± 0.61	9	31 ± 1.02	21	4.3 ± 0.33
WW	12	2 ± 0.0	2.6 ± 0.15	12	32.8 ± 1.32	12	1.7 ± 0.14
M DA	8	1.25 ± 0.16	2 ± 0.0	2	32.6 ± 1.45	8	3.3 ± 1.75
M BA	8	2 ± 0.0	2.3 ± 0.16	8	33.3 ± 1.28	8	2.3 ± 0.34

(SW) Slow Wave, (WW) Waxing Waning, (M DA) Mucosa Decanoic acid, (M BA) Mucosa Butyric acid
(LF) low frequency, (HF) high frequency
Frequency components refers to how many frequency components isolated
N(exp) states how many experiments of total N displayed previous frequency component
WW contains data from DA induced and spontaneous instances of waxing waning

are from recordings of spontaneous waxing waning in addition to DA induced (Table 3.1).

In preparations where a steady slow wave was present in the control, addition of 10 mM amino acid mix (5 mM L-tryptophan, 5 mM L-phenylalanine) failed to induce any waxing waning like electrical activity. It was concluded amino acids do not induce the waxing waning pattern on circular smooth muscle preparations.

Addition of 10 mM BA to circular muscle preparations did not induce the waxing waning phenomenon; however it did have an effect on the slow wave exhibited by smooth muscle cells. BA decreased the duration of the slow wave ($n=5$, $p<0.05$, mean 190 ± 58 ms). There was no change to the frequency or amplitude parameters.

3.3.2 Hemi-dissected preparation

With the use of the partitioned chamber and hemi-dissected preparation, reagents could be added to the half of the dish housing the mucosa intact portion. The reagent did not cross the barrier or come in contact with the exposed circular muscle being recorded from. 1 mM DA applied to the mucosa was unable to induce a visual waxing waning pattern ($n=8$, Fig 3.9). In three experiments, when DA applied to the mucosa had no response within 40 minutes, DA was then perfused onto the circular muscle half of the chamber as a positive control. This resulted in a visible waxing waning pattern ($n=3$). To determine if any low frequency activity was induced, wavelet analysis was performed on each experimental stage. Wavelet analysis picked up a low frequency component in two experiments that persisted from the control to the addition of DA. However the low

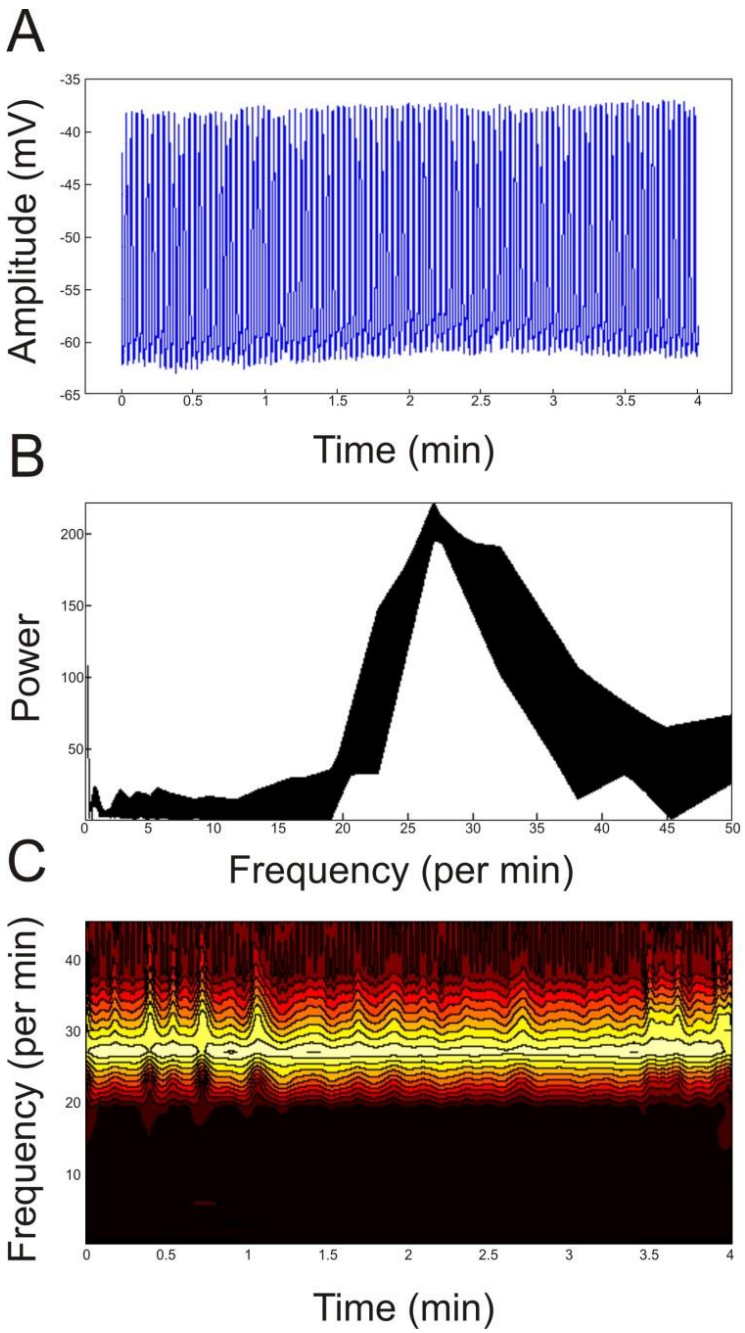

Figure 3.9 Frequency components after mucosal application of DA. Intracellular electrical activity of circular muscle after 1 mM DA (A). Continuous wavelet transformation analysis shows frequency distribution of source (B). Time-frequency contour plot of mean power (continuous wavelet transform analysis) shows a high frequency component (C).

frequency component was too weak and inconsistent; the HF:LF ratio was always above 3.0 (n=2, mean 5.0 ± 1.1) and thus did not influence the slow wave pattern. The addition of DA to the mucosa never induced onset of additional low frequency components nor waxing waning.

When 10 mM BA was applied the circular muscle directly, no change in slow wave pattern was detected. However when 10 mM BA was perfused to the mucosa, five of eight experiments observed an obvious change in the SW pattern, similar to waxing waning (Fig 3.10). The time required for the change in pattern varied among preparations (n=5, mean 19.94 ± 3.22 min). The reason the pattern is similar to, but not quite waxing waning is due to the irregularity of the pattern and the amplitude of the slow wave during wanes were generally greater than 50% of the amplitude during waxing (Fig 3.10A). Although the waxing waning like pattern was only visually obvious in 5/8 experiment post addition of BA, wavelet analysis determined perfusion BA always induced a low frequency component (Table 3.1).

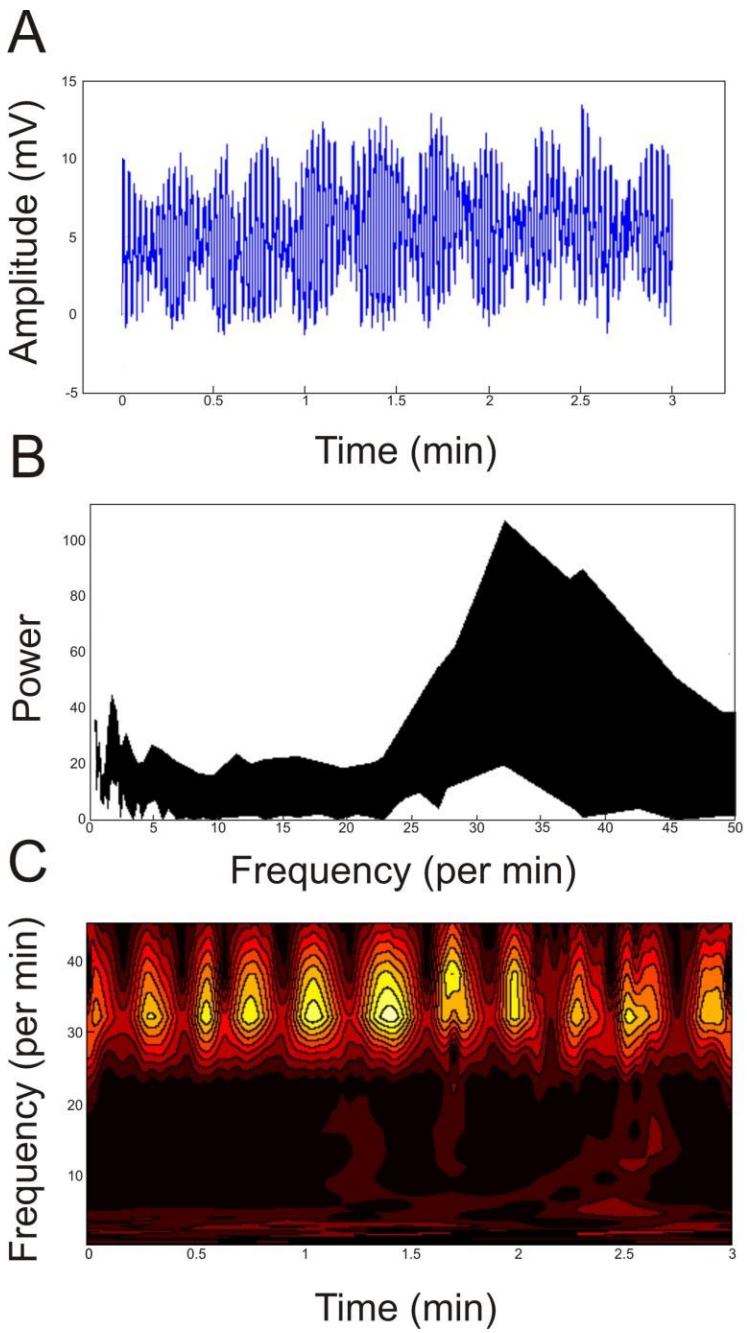

Figure 3.10 Frequency components after mucosal application of BA. Intracellular electrical activity of circular muscle after 10 mM BA (A). Continuous wavelet transformation analysis shows frequency distribution of source (B). Time-frequency contour plot of mean power (continuous wavelet transform analysis) depicts the presence of a high frequency and a low frequency component (C).

3.4 Discussion

The phenomenon of the waxing waning electrical pattern is extremely interesting to study, as it may provide insight at the cellular level to the mechanisms initiating the segmentation motor pattern in the small intestine. Occasionally, the waxing waning pattern can be observed from smooth muscle cells without prior experimental stimulation. In these conditions neural inhibitors, TTX and atropine, were unable to abolish, or modify the phenomenon in any way. This is strong evidence suggesting once the waxing waning pattern is initiated it is under myogenic control. 1 mM DA was used by Gwynne and Borstein (2004) to induce segmentation in the guinea pig small intestine *in vitro* in an organ bath. The same concentration applied to circular muscle pinned flat for intracellular recording in a small bath induced rhythmic waxing waning behaviour identical to that initially recorded by Bortoff (1965). Experiments revealed DA induced waxing waning was initiated in the presence of TTX, proposing the waxing waning pattern can be initiated solely by myogenic pacemakers. However, this is not to say waxing waning can't be initiated by the ENS; it merely states certain stimuli can evoke the pattern without ENS influence.

The experimental results of most interest in these studies were the almost opposite effects of DA and BA on exposed circular muscle, and on mucosa intact preparations. When 1 mM DA was perfused onto exposed circular muscle preparations a low frequency component (mean 2.6 ± 0.15 opm; Table 3.1) resolved and a rhythmic waxing waning pattern emerged from a steady slow wave. 10 mM BA on the same preparation did not

evoke the low frequency component or induce waxing waning, but did decrease the duration of the slow wave.

However, when DA was perfused onto the mucosa intact preparation no response was elicited. In these hemi-dissection preparations the addition of BA always induced the low frequency component (mean 2.3 ± 0.16 opm; Table 3.1), and introduced a slightly irregular waxing waning like pattern from the existing slow wave in five of eight experiments. As mentioned previously, BA induced waxing waning was not as rhythmic as that evoked by DA, and the waning amplitude of the slow wave was generally greater than 50% of the waxing slow wave. The aforementioned aside, the visually observed electrical oscillations were clearly similar to waxing waning, and a low frequency component was present.

To shed some insight into why these discrepancies occurred, each nutrient was investigated. A MCFA such as DA (otherwise known as capric acid) is a ten carbon chained fatty acid usually contained in triacylglycerol found in general foods at low concentrations. These include butter, cream, milk (2-3%), and in palm kernels and coconut oils (7%, 14% respectively) (Takeuchi et al., 2008, Zentek et al., 2011). Medium chain triacylglycerols are hydrolyzed to fatty acids and glycerol by pancreatic triglyceride lipases (Takeuchi et al., 2008, Nutting et al., 2002). Free form MCFAs are absorbed by passive diffusion into the portal blood where they are bound with albumin and transported to the liver where they are oxidized into ketones and carbon dioxide (Takeuchi et al., 2008, Nutting et al., 2002, Zentek et al., 2011). It is believed MCFAs can permeate through a paracellular route, the aqueous pathways in the intracellular space between

adjacent cells (Cano-Cebrian et al., 2005). Interestingly decanoate is able to modulate paracellular permeability by increasing intracellular calcium levels through activation of phospholipase C (PLC). Activated PLC cleaves phosphatidylinositol 4,5-bisphosphate into IP3 and diacyl glycerol, the former of which releases calcium from intracellular stores and facilitates contraction (Lindmark et al., 1998). It is possible DA induces the low frequency component by stimulating PLC activity in the responsible oscillatory cell.

Recent calcium imaging data from our lab (Huizinga et al., submitted August 2013 to Nature Communications) found addition of 1 mM DA modified calcium activity of ICC-DMP to produce a low frequency oscillatory pattern (4 opm). Perhaps DA applied to the circular smooth muscle activates PLC in ICC-DMP subsequently triggering a signalling cascade to evoke low frequency activity. In the hemi-dissected preparations, addition of DA failed to introduce a low frequency component, and thus the rhythmic waxing waning pattern. It is plausible DA and MCFAs are unable to induce the low frequency component unless a significant concentration comes in contact with the circular muscle layer. Free form fatty acids are not degraded at the level of the mucosa but instead diffuse into the portal blood where they are metabolized in the liver (Takeuchi et al., 2008). In these preparations there is very little blood flow and it is possible DA is unable to interact with the circular muscle or ICC-DMP populations as it might *in vivo*.

In the colon, butyric acid (a common component of colonocyte cellular metabolism) is predominantly taken up by colonic epithelium and metabolized to produce energy (Guilloteau et al., 2010). Butyrate is absorbed in the small intestine by similar mechanisms to that in the colon. Generally BA can be transported into enterocytes via

non-ionic diffusion (SCFA/HCO3 exchanger), by a monocarboxylate transporter (MCT type 1) or through Na coupled monocarboxylate transporter (SMCT or SLC5A8/12) (Guilloteau et al., 2010). Interestingly, BA can be entirely metabolized in these cells. This is likely why BA perfused onto the circular muscle preparations was unable to induce a low frequency response. On the other hand, because the action of BA is at the level of the mucosa, this is precisely why it was able to induce waxing waning and the low frequency component in the five of eight hemi-dissected preparations. While the mechanism by which BA induces the low frequency component can currently only be speculated upon, it may involve after hyperpolarization neurons. Kunze et al. (2009) found a spritz of 5 mM butyrate on the mucosa in the rat colon induced a non-synaptic burst of action potentials in these sensory neurons. Thus primary afferent sensory neurons may play a role in stimulating the low frequency component in response to the chemical stimulant butyrate.

The 10 mM mixture of amino acids (L-tryptophan and L-phenylalanine) perfused onto circular muscle tissue was unable to stimulate the low frequency component or the waxing waning pattern. This was interesting as Gwynne and Borstein (2004) found that these amino acids were able to induce segmental contractions in the guinea pig organ bath. A key difference between experiments was the concentration used. They used 30-50 mM of amino acid mixture to induce their response. The 10 mM used may have been too weak a concentration to induce the low frequency response. 30 mM could be used in the future to confirm the results.

4. ISOLATION OF THE LOW FREQUENCY COMPONENT

4.1 Introduction

Recent data from our lab (Huizinga et al., submitted August 2013 to Nature Communications) reveals low frequency calcium oscillations in the ICC-DMP networks after stimulation with 1mM decanoic acid. This was reasonable evidence implicating ICC-DMP as the initiator of the low frequency activity isolated via CWT in the previous chapter. A large problem faced when attempting to observe low frequency activity is the strong dominant presence of the omnipresent slow waves originating from the ICC-MP networks. In order to observe the uninfluenced low frequency activity, and to prove it itself is not produced by the ICC-MP it was necessary to abolish the ICC-MP activity.

The small intestine of c-Kit deficient W^v mutant mice is incredibly attractive to study due to their lack of ICC-MP networks, and thus intestinal slow waves (Huizinga et al., 1995). Mutations on the white spotting locus W, which encodes the Kit protein kinase receptor, results in a complete loss of activity (W allele) or severely diminished activity (W^v allele) of the Kit protein present in ICC (Malysz et al., 1996). With very low levels of the active Kit protein, the interaction between Kit and the steel factor during ICC development is absent, thus ICC-MP networks fail to develop (Torihashi et al., 1995).

Interestingly, these mice survive and mature into adulthood despite lacking the pacemaking system of the small intestine. The lack of ICC-MP networks in these mutant mice significantly decreases transit time of bowel content (Hou et al., 2005, Huizinga et

al., 1999). Irregular action potential activity has been consistently reported in the literature in place of slow waves (Huizinga 1999, Nakagawa et al., 2005, Malysz et al., 1996). Increasing pressure in the W^v small intestine has been shown to evoke a low frequency (2.5 contractions per minute) aborally propagating rhythmic burst activity of action potentials (Nakagawa et al., 2005). This activity was abolished with neural blockade. Clearly the W^v mouse small intestine possess the mechanisms to produce rhythmic low frequency contractile activity in the absence of ICC-MP networks.

Generally, visible pacemaker (slow wave) activity in these mice is completely absent. However, in an *in vivo* study by Hou et al. (2005), extracellular electrodes picked up rhythmic slow waves of a significantly lower frequency and amplitude than wildtype slow waves (11 opm). In W^v mutant mice ICC-DMP networks are morphologically unaffected by the mutation and thus are the prime suspects in the generation of rhythmic oscillations (Hou et al., 2005).

Although W^v mice may appear to be prime models to investigate the low frequency component without the influence of a dominant high frequency component, there could be many unaccountable variables. The circular muscle layer of the W^v mouse has highly irregular action potential and there is rhythmic longitudinal muscle activity (Huizinga et al., 1999). Additionally, morphological studies can't determine any adaptions made by other cell types in the myenteric plexus, such as fibroblast like cells, which may have developed differently in response to the lack of ICC-MP networks to fulfill a similar role. It may be necessary to induce the loss of ICC-MP in a short time frame to prevent adaptive measures.

Lui et al. (1994) used the nerve dye methylene blue (MB) to abolish ICC-MP activity. Incubation of canine colonic circular muscle preparations with the dye absorbed into all cells and was subsequently washed out. Interestingly, ICC-MP retained the dye and intense illumination (subsequent to the wash) physically damaged ICC mitochondria resulting in cell death, a loss of network connectivity, and thus loss of slow wave generation. Electron microscopy revealed no physical damage to the ICC-DMP networks. In this chapter MB mediated destruction of ICC-MP was utilized to examine low frequency activity.

4.2 Methods

Intestinal jejunum segments from adult female WBB6F1 J homozygous (wildtype), WBB6F1/J-Kit^{W}/Kit^{W-v}/J (W^{v}), and CD-1 mice were used for intracellular recording experiments. Information regarding animal handling and intestinal excision can be found in section 2.1 and 2.2 respectively.

4.2.1 W^{v} experiment proper

W^{v} experiments generally followed the same course of procedures as outline in section *3.2.1,* however segments of the ileum were utilized instead of jejunum. In all preparations, controls were obtained by recording uninterrupted electrical activity for a period of at least five minutes from a single circular smooth muscle cell. Extra care was taken with recordings from the W^{v} small intestine as no slow wave exists as a marker to determine if a smooth muscle cell was penetrated properly. Generally, successful recordings were observed as a fluctuating baseline. To ensure the microelectrode was correctly inserted and recording from a smooth muscle cell, the voltage must zero after the electrode is pulled out. This limited continuous recordings to a maximum of four minutes. After a four minute control recording, 1mM DA was then added to the inflow reservoir of fresh Krebs' solution and subsequently perfused on the tissue samples.

4.2.2 High frequency annihilation experiment proper

To abolish the high frequency ICC-MP slow wave, methylene blue dye was used following the same procedure as Liu *et al.* (1994). After a five minute control recording

methylene blue was perfused onto a circular muscle tissue preparation (*3.2.1*) in the absence of light for duration of 10 minutes. The tissue was subsequently washed with Krebs' solution for five minutes, followed by intense illuminated via a fiber optic cable (115 V, 50-60 Hz, 11 W, Helmut Hund GmbH, Wetzlar, Germany). Once the slow wave was abolished normal light was restored and DA was perfused onto the preparation.

4.2.3 Data analysis

Raw data was collected and analyzed as described previously in section *3.2.3*. Frequency, amplitude, and duration parameters were not calculated for W^v experiment data.

Supplemental to CWT analysis, to visualize low frequency components original raw data was subjected to a Bessel (8-pole) lowpass with a -3 dB cutoff of 0.1 Hz using Clampex 9.2 software (Molecular Devices). This eliminated all frequency sources above the cut-off, leaving only low frequency electrical activity.

4.3 Results

4.3.1 Wv circular muscle preparation

In prior circular muscle preparations nicardipine was added to the Krebs' solution to paralyze the tissue and prevent muscle contraction which would detrimentally affect microelectrode recordings. However, the W^v mutant tissue preparations which lack ICC-MP networks did not display rhythmic slow wave associated muscle contractions and thus did not require paralysis.

The c-Kit knockout mice presented a substantial challenge while recording. The circular muscle lacks ICC-MP driven slow waves which are usually sought out to determine if the electrode has successfully penetrated a single cell. It was extremely difficult to ascertain if the electrode was recording from a stable cell when the resting membrane potential dropped to the voltage of a biologically active muscle. The only conclusive way to determine the microelectrode was in fact recording was to remove the electrode and observe whether or not the voltage returns to zero (as it would if the intracellular electrode and recording electrode were in the same medium). Figure 4.1A illustrates an intracellular recording from circular muscle of a W^v mouse. The recording consists of a fluctuating baseline hovering around the approximate resting membrane potential of ~45-50 mV a smooth muscle cell.

Addition of 1 mM DA in induced short term bursts of inhibitory junction potentials (IJPs) in five of seven preparations, and in rare cases was associated with

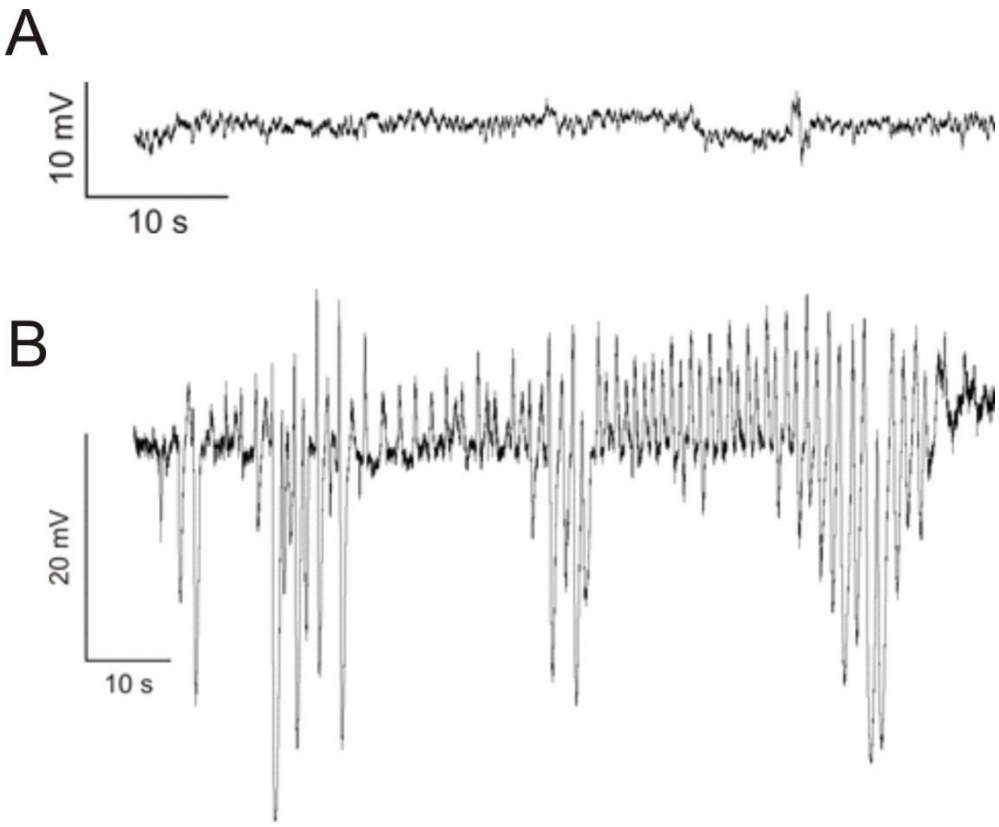

Figure 4.1 Intracellular recording from circular muscle of a W^v mouse. The knockout mouse lacks slow wave activity; only small fluctuations can be seen at a baseline RMP of ~ -45 to -50 mV (A). In rare cases after addition of 1 mM DA induced short term bursts of IJPs and slow wave like activity at a frequency of 50 min^{-1} (B).

high frequency slow wave like activity (n=3, mean 13.3 ± 3.77 min; Fig 4.1B). In this pattern, a mix of IJPs and pseudo slow waves, the slow waves occurred at an extremely high frequency (n=3, mean 43.7 ± 3.48 opm), was observed. In Fig 4.1B, the first IJPs prior to the initiation of the pattern may have caused post inhibitory excitation which would be able to significantly depolarize the cell and allow rhythmic excitatory activity to follow. These bursts of IJPs and pseudo slow waves were usually short lived rarely lasting more than one minute.

CWT analysis of recordings from the W^v mouse detected a low frequency component in almost all recordings (Table 4.1, Fig 4.2). Generally, the addition of 1mM DA did not result in any visibly sustained electrical pattern, however CWT analysis picked up a slight increase in oscillatory activity at a range of different frequencies (Table 4.1). The short lasting IJP activity mentioned earlier is composed of multiple frequency components (Fig 4.2F). It is interesting to note, in the frequency-time contour map the low frequency component is visible before and during the IJP burst. Evidence provided in Figure 4.2 suggests the low frequency component in omnipresent in W^v mice.

Control experiments were performed on ileal segments of wildtype mice. In all but one experiment (n=6), 1 mM DA failed to induce waxing waning within half an hour of application. This was unfortunate, as the ileal tissue of the wildtype control mice were not as responsive to DA stimulation as the jejenum of CD-1 mice in the nutrient study.

Table 4.1 Analysis of Frequency Components the W^v Mouse

Experimental stage	N	# Frequency Components	LF (mean)	N(exp)	HF (mean)	N(exp)
Control	7	1.1 ± 0.14	3.9 ± 0.40	7	16.0	1
DA	7	1.3 ± 0.26	4.2 ± 0.66	6	19.9 ± 3.4	3

(DA) Decanoic acid, (LF) Low Frequency, (HF) High Frequency
Frequency components refers to how many frequency components isolated
N(exp) states how many experiments of total N displayed previous frequency component

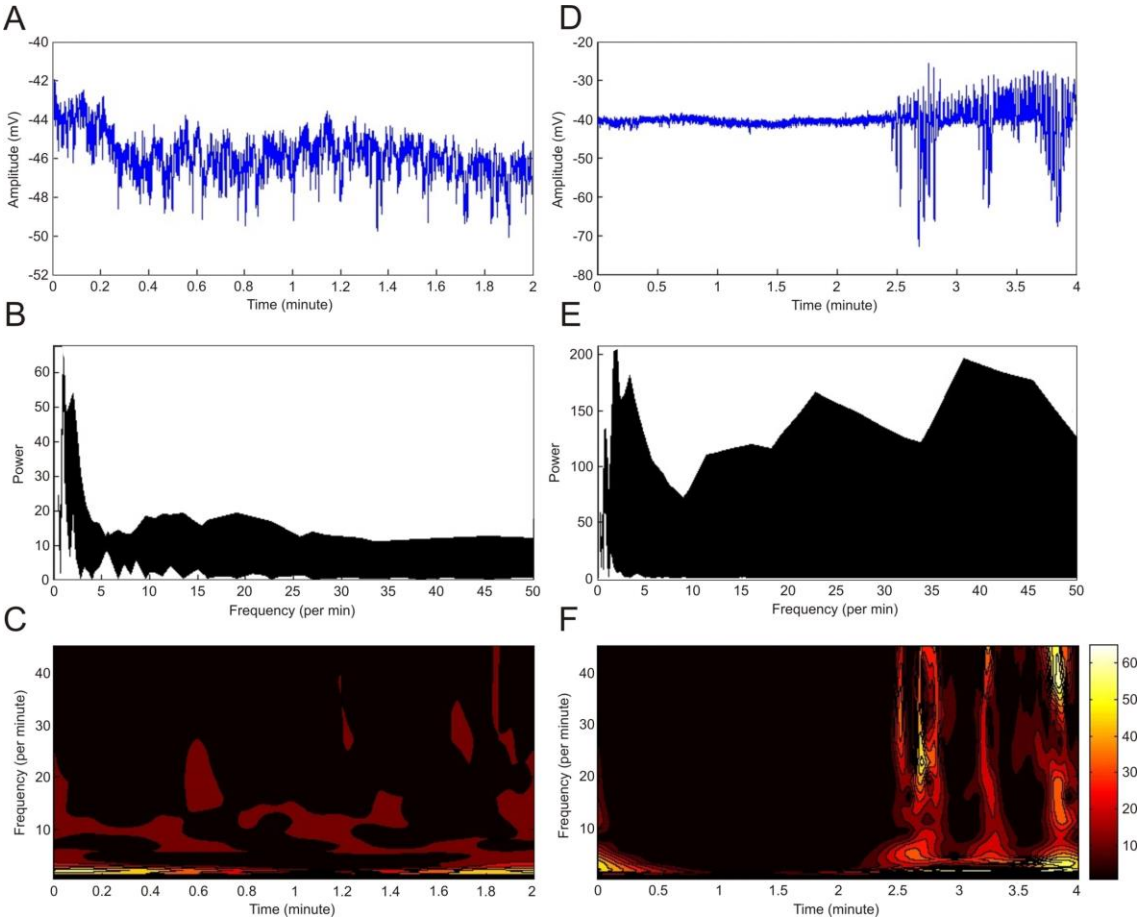

Figure 4.2 Frequency components in the W^v mouse. CWT analysis of W^v electrical activity depicts the omnipresence of the low frequency component during control conditions (ABC), and after perfusion of 1 mM DA (DEF). Visual low frequency oscillations were difficult to detect by observation of voltage time graph (A). Power spectrum analysis (B) and the frequency over time contour map (C) demonstrate the presence low frequency activity with accompanied sporadic higher frequency activity. In the rare case of short term IJPs and high frequency oscillations post DA (D) Power spectrum (E) analysis and the frequency over time contour map (F) both determined the low frequency component was present prior to and during the burst activity. High frequency activities of variable frequencies were associated with the burst activity.

4.3.2 High frequency annihilation

The W^v mouse may not be the best model to study the low frequency component without the influence of the high frequency component. Developmental adaptations could have surfaced to compensate for the loss of ICC-MP activity. It became essential to eliminate the dominant high frequency component (the slow wave) in the shortest amount of time to prevent adaptation and the emergence of uncharacterized frequency components. To achieve this annihilation of the slow wave, circular muscle tissue preparations of CD-1 mice exhibiting a slow wave were incubated with MB, washed, and subsequently exposed to intense fibre optic illumination. This illumination was sufficient to eliminate the high frequency slow wave component. The aim was to provide a low influence environment to characterize the low frequency component being sought.

Analysis of the MB experiment clearly depicts a story (Table 4.2). During the control, MB incubation, and MB wash experimental stages a high frequency component is present. However, as the experiment progresses the slow wave gradually diminishes in amplitude until extinction. Once the slow wave was completely annihilated only one of four preparations still displayed a low frequency component. After abolition of the slow wave 1 mM DA was perfused onto the quiescent tissue in attempt to stimulate the low frequency component (Fig 4.3). In four of five experiments with successful intracellular recordings during the DA stage, the low frequency component (mean 2.75 ± 0.48 opm) was resolved. It is important to note, the low frequency component was not visually apparent while recording from the smooth muscle tissue, and could only be consistently

Table 4.2 Analysis of Frequency Components during High Frequency Annihilation

Experimental step	N	LF (mean)	N(exp)	HF (mean)	N(exp)	HF:LF
Control	6	3.25 ± 0.75	2	28.7 ± 1.05	6	3.25 ± 1.75
MB	5	3.33 ± 0.89	3	28.5 ± 1.43	5	4.33 ± 0.33
MB Wash	3	5	1	24.5 ± 0.96	4	6
Illum No SW	4	7	1	NP	0	N/A
DA	5	2.75 ± 0.48	4	NP	0	N/A

(MB) Methylene Blue, (Illum) Illumination, (SW) Slow wave, (DA) Decanoic acid, (NP) Not Present
(N/A) Not Applicable
Frequency components refers to how many frequency components isolated
N(exp) states how many experiments of total N displayed previous frequency component

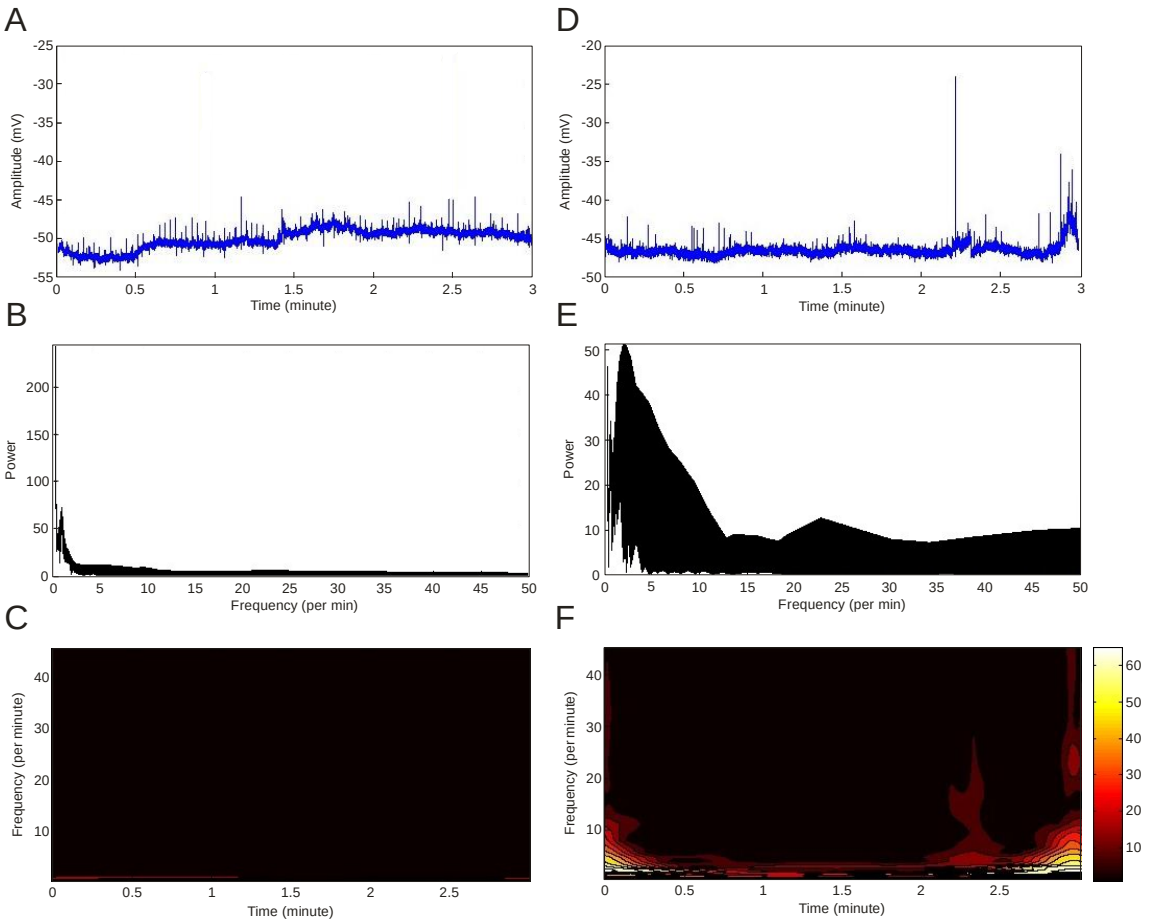

Figure 4.3 Frequency components after methylene blue mediated disruption of ICC-MP networks. Loss of electrical activity after intense illumination (ABC), and subsequent addition of 1 mM DA to quiescent tissue (DEF). Electrical activity of quiescent circular muscle (A). Power spectrum frequency distribution of source depicts complete loss of oscillatory components (B). Time-frequency contour plot shows the lack of frequency components through time (C). Intracellular electrical activity of circular muscle after addition of 1 mM DA (D). Power spectrum frequency distribution of source depicts a low frequency component (E).Time-frequency contour plot shows the strength of the low frequency component through time (F).

isolated when wavelet analysis was conducted on voltage-time recordings.

In addition to CWT analysis, raw data was filtered to visualize low frequency component in the voltage time domain. From the same raw data used in Figure 4.3D, the low frequency electrical oscillatory activity could be observed (Fig 4.4). The low frequency oscillations are very small in amplitude, barely exceeding 1 mV. Obvious low frequency activity such as was only observed in a minuscule sample of all recordings. This is because any fluctuation in the resting membrane potential masked the oscillations.

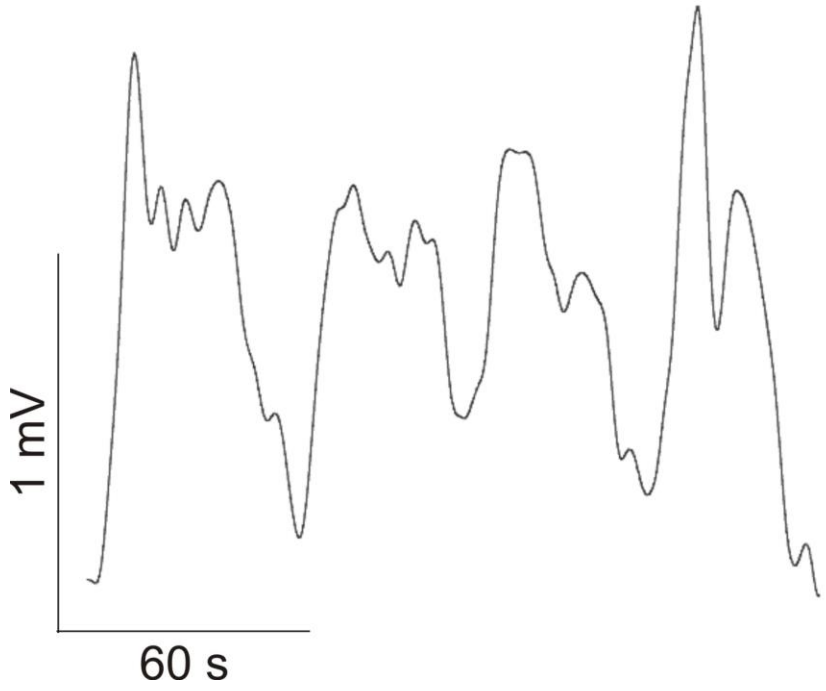

Figure 4.4 Low frequency component after low filter bypass. Data obtained from addition of 1 mM DA after methylene blue mediated slow wave annihilation. All frequency components above 0.1 Hz were filtered to observe the low frequency component from intracellular electrical recordings.

4.4 Discussion

W^v mice were first investigated in attempt to isolate and study the low frequency component without the influence of the dominant high frequency component. Perfusion of DA onto the ileal preparation failed to produce a visual low frequency component. CWT analysis revealed the low frequency component was omnipresent (3.9 ± 0.40 opm). In the W^v mice, the ICC-DMP populations are still intact. It is possible these cells are always active in the mutant mouse to compensate for the lack of slow wave activity.

Control recordings from ileal segments of the wildtype mouse did not respond to DA application. This was an unfortunate result to obtain after conducting experiments on the W^v mouse. It should be noted the original inquisitive study by Gwynne et al. (2004) on the effects of DA found the ileum to be least responsive to the medium chain fatty acid (compared to duodenum and jejunum). It is believed MCFAs rarely reach the ileum *in vivo* with significant concentration to exert an effect. This is because they are rapidly absorbed in the duodenum and jejunum (Takeuchi et al., 2008, Nutting et al., 2002, Zentek et al., 2011). Conducting the experiment with a tissue segment from the jejunum would likely have yielded a different result; however due to sharing of tissue by all lab members, the ileum was all that could be spared of the small intestine to examine.

Although the ICC-MP populations are lost in the c-Kit knockout, W^v mice are able to survive into adulthood. The lack of the dominant pacemaker system results in decreased GI transit time. However, some adaptations might have occurred during development to compensate for the lack of pacemaker system. One example may be the

high frequency rhythmic longitudinal muscle contractions observed in W^v small intestine organ bath study by Marc Pistilli (2012, data unpublished; Fig 4.5). The rhythmicity of these high frequency contractions are very similar to ICC pacemaker activity and thus prompted literature investigation into ICC-MP progenitor cells which could have resulted in the development of a pseudo pacemaking system.

In the W^v mice, fibroblast like ICC (FL-ICC) have been identified having gap junction contact with the smooth muscle layers, and with other FL-ICC (Lorincz et al., 2008, .Kazuhide et al., 2000). These cells are distinguishable from other fibroblast due to their high electron density cytoplasm and well developed rough endoplasmic reticulum (Kazuhide et al., 2000, Wang et al., 2009). FL-ICC are identified as ICC progenitors based on expression of ICC markers: c-Kit, insulin like growth factor 1 receptor (Igf1r) and CD34 (Wang et al., 2009). Where ICC-MP would reside in the Wv mice, FL-ICC were found positive for CD34 and Igf1r suggesting FL-ICC are the matured progenitor form. However, with all the aforementioned evidence, FL-ICC are unlikely the cells responsible for the rhythmic contractile activity observed in our lab and by others because there is no evidence of increased populations compared to the wild type mouse (Wang et al., 2009)

ICC-MP and longitudinal muscle originate from a common precursor cell expressing c-Kit, and diverge at E14/E15 (Wang et al., 2009, Kurahashi et al., 2008). During development ICC-MP and longitudinal muscle both express PDGFrα, PDGFrβ,

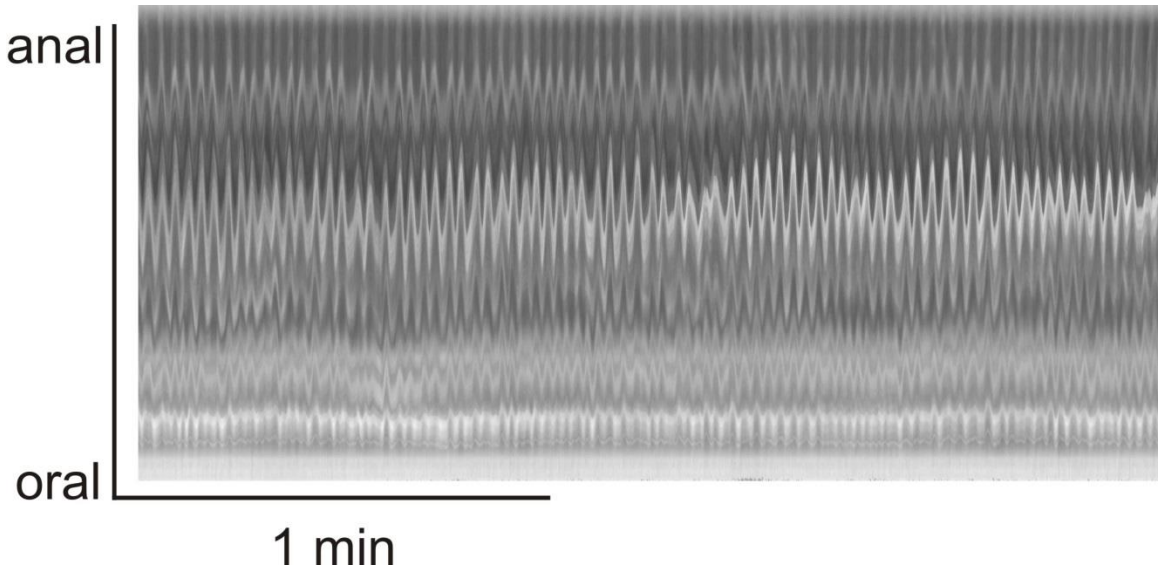

Figure 4.5 Organ bath spatio-temporal map of W^v small intestine. Darker regions of the map demonstrate a narrowing of the lumen and are associated with contraction. White areas on the other hand represent a non-occluded lumen. Rhythmic longitudinal contractions present in the small intestine of the W^v mouse without external stimulation. Image courtesy of Marc Pistilli, 2012.

and c-Kit at E13, before they differentiate (Kurahashi et al., 2008). Unlike the ICC-MP and the longitudinal muscle, circular muscle cells do not express any PDGF receptors and thus are unlikely to pace themselves (Kurahashi et al., 2008). It is plausible the longitudinal muscle in W^v mice are capable of pacemaking activity. Unfortunately, intracellular recordings from the longitudinal muscle of W^v ileal tissue preparation revealed no evidence of rhythmic depolarizations observed in the organ bath (n=4, data not shown). Perhaps the reason the rhythmic longitudinal muscle activity was not observed was due to the small 1 by 1 cm preparation size; rhythmic contractions may require a larger group of smooth muscle cells to pace. If indeed the longitudinal muscle cells are responsible for pacing themselves in the W^v mouse intestine, it would be necessary to record electrical activity from them alone, without the influence of cells in the myenteric plexus. A way to avoid meticulous peeling/separation of layers would be to culture the longitudinal muscle cells and utilize both intracellular recording and patch clamping techniques to determine if they possess their own myogenic pacing mechanism.

While these developments are interesting themselves, they represent many variables that can't be accounted for when trying to induce and isolate a low frequency component. Methylene blue was used to abolish the high frequency slow wave in a short time frame, thus preventing adaptation. The control stages of the methylene blue were all satisfactory. There were no significant changes to any slow wave parameter during the addition of methylene blue or the subsequent wash. Once the slow wave was abolished very little activity was picked up during CWT analysis. The presence of a low frequency oscillator during illumination of one experiment maybe explained: a) the low frequency

component is always present at basal levels, but is dominated by the high frequency component; b) the loss of the high frequency component was gradual, and thus local ICC-MP pacemaking populations within the network may have been inhibited at different rates thereby causing a disturbance in the network; or c) illumination may have directly or indirectly stimulated the low frequency pacemaker.

Addition of 1 mM DA produced a small amplitude low frequency component. This is strong evidence DA induces the low frequency pacemaker. Unfortunately, this low frequency component was rarely observed visually in the voltage time electrical recordings. After a low filter bypass the low frequency component could be observed as small 1 mV fluctuations. This may mean the low frequency component's influence is subtle and likely manipulates the high frequency component through a phase-amplitude coupling during waxing and waning of the high frequency component. This idea arose from the interaction between the theta oscillations and gamma waves in the hippocampus (Belluscio et al., 2002). The phase of the low frequency theta waves (4-7 Hz) couples with the amplitude of the high frequency gamma rhythms (25-150 Hz), thus phase-amplitude coupling. Parallel to the hippocampus, it is likely the low frequency component induces waxing waning by coupling with the high frequency signal from the ICC-MP in the circular muscle. The cellular mechanisms responsible for its activation or inhibition are currently unknown and can only be speculated. ICC-DMP do not retain MB, the dye is washed out of these ICC as well as the surrounding smooth muscle during the washout step. It is likely the ICC-DMP network is responsible for the low frequency component.

5. ICC-DMP Pharmacology

5.1 Introduction

There hasn't been a lot of success in conclusively identifying the role of the ICC-DMP in the small intestine. While evidence exists for physical contacts between ICC-DMP and excitatory and inhibitory nerves, as well as smooth muscle cells, there is no concrete data of ICC-DMP in action (Wang et al., 2003, 2005; Lee et al., 2009; Iino et al., 2006). Recent evidence from our lab (Huizinga et al., submitted August 2013 to Nature Communications) has revealed low frequency calcium oscillation activity in individual ICC-DMP cells at a similar frequency to the low frequency component identified in waxing waning. While little is known of the role of ICC-DMP in the small intestine, a substantial amount of information exists on the myogenic low frequency component in the colon.

Many studies on human, canine, and murine models have demonstrated two rhythmic myogenic oscillators exist in the colon (Bueno et al., 1980, Pluja et al., 2001, Smith et al., 1987, Yoneda et al., 2002, Liu and Huizinga 1993). In the canine model it was found that the two dominant frequency components reside in two different plexuses; the low frequency high amplitude (LFHA) component originated from the submuscular plexus, and the high frequency low amplitude (HLFA) component originated from the myenteric plexus (Smith et al., 1987, Lui and Huizinga 1993). These two signals propagate through the circular smooth muscle layer and appear interact via summation. Intracellular recordings from cross sections of the circular muscle layer adjacent to either

plexus (myenteric plexus and submuscular plexus) were predominantly at the frequency of the nearby oscillator. However, the middle of the muscle thickness was clearly influenced by both the oscillators, the HFLA superimposed on the LFHA (Fig 5.1). It was hypothesized this superimposition of signals facilitates a greater depolarization than each would individually thereby increasing the signal strength (Smith et al., 1987).

The murine model differs slightly from the larger mammal models (canine and human). The origin of both HFLA and LFHA oscillations appear to originate from opposite plexuses. The HFLA resides in the submuscular plexus and the LFHA from the myenteric plexus (Pluja et al., 2001, Yoneda et al., 2002, 2004). Controversy existed over the origin of the low frequency depolarizations and was headed by two opposing ideas. The first suggested it was a neurogenic mechanism partially resistant to calcium channel blockers, while the second proposed ICC-MP were the rhythmic pacemakers responsible for creating LFHA oscillations (Pluja et al., 2001). Similar to the ICC-MP slow wave of the small intestine, the HFLA is myogenic; able to continue functioning without alteration in the presence of TTX (Pluja et al., 2001). Interestingly, TTX and similar neural inhibitors do not abolish the LFHA component but instead increase its frequency and amplitude (Pluja et al., 2001, Benabdallah et al., 2008, Dickson et al., 2009). Nω-nitro-L-arginine (L-NNA), a nitric oxide synthase inhibitor, also increases the frequency of LFHA oscillations (Kato et al., 2009). This implies the LFHA oscillator is not a true myogenic pacemaker, and is under tonic inhibitory neural control.

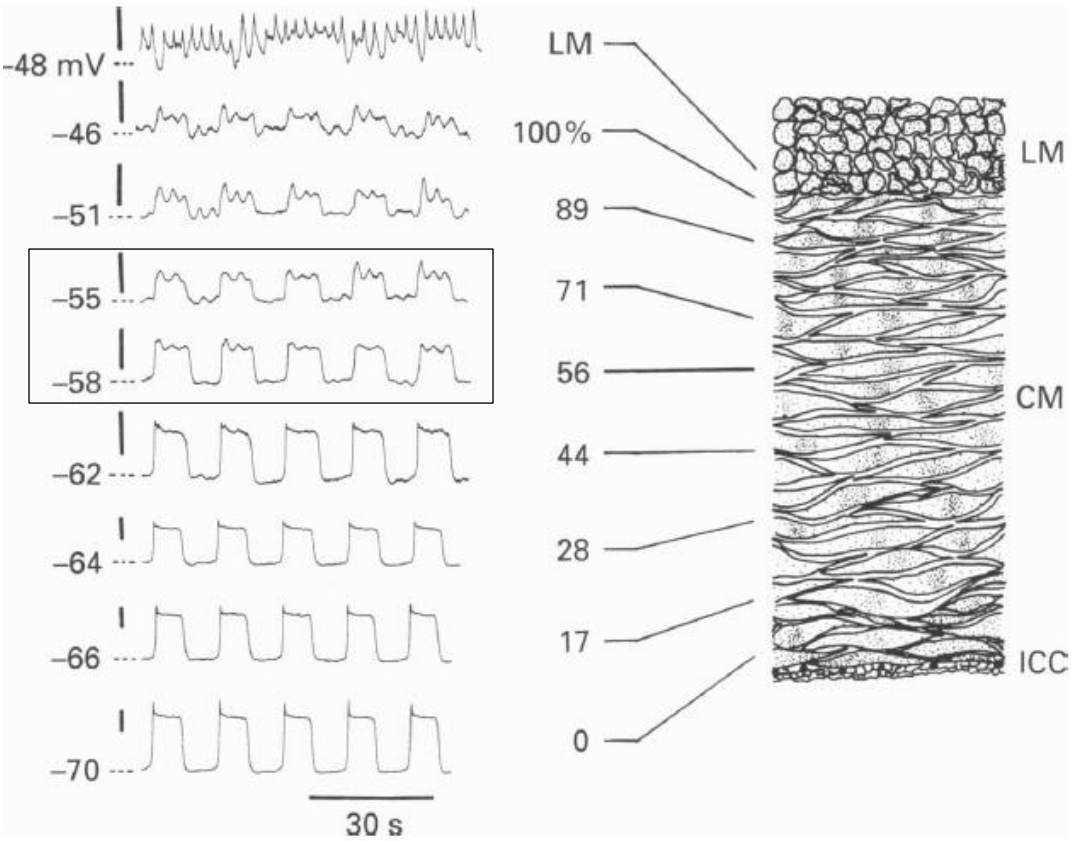

Figure 5.1 Intracellular recordings through the canine circular muscle thickness. Distances were normalized as a percentage: 100 % refers to microelectrode impalements of circular muscle directly by the myenteric plexus, while 0 %, indicated a recording directly by the SMP. Percentages correlate to their location in the muscle thickness between the two plexuses. The interaction between the two pacemakers is best seen in the [boxed outline] which clearly demonstrate the high frequency oscillations superimposed on the low frequency oscillations. Figure adapted from Smith et al. (1987).

In the small intestine waxing and waning of single cell electrical activity is the only evidence of high frequency component (ICC-MP slow wave) and low frequency component interaction as of yet (see section 3 and 4). The ICC-DMP form close synaptic contacts with excitatory (cholinergic, tachykinergic) and inhibitory (nitrergic) nerves (Wang et al., 2003). Three dimensional modeling of ICC-DMP electron microscopy sections revealed ICC-DMP processes encircle enteric nerves (in close proximity) and invaginate circular smooth muscle cells (Lee et al., 2009). These physical connections as well as shared gap junctions between adjacent ICC-DMP and smooth muscle cells are supportive evidence for the hypothesis in which ICC-DMP act as neural mediators, or as an alternative route for neuromuscular transmission (Wang et al., 2003, Lee et al., 2009). It is possible some parallels can be drawn from the neurally regulated LFHA generating ICC of the colon to the ICC-DMP of the small intestine.

ICC-DMP expresses strong NK1r immunoreactivity, indicating they can be influenced by SP (the excitatory tachykinin which has the highest affinity for NK1r) the most represented tachykinin in the gut (Faussone-Pellegrini 2006, Iino and Horiguchi 2006, Shimizu et al., 2008). The close physical proximity of tachykinergic nerves to ICC-DMP cells is strong evidence for excitatory control of the ICC networks via diffusion of the SP neurotransmitter into the intercellular space after synaptic release (Faussone-Pellegrini 2006).

SP and NK1r signalling is regulated to prevent over stimulation by internalization (Kilwood et al 2001). Receptor ligand complexes are internalized in the post-synaptic cell

(ICC-DMP) where the ligand is degraded and the receptor is either degraded as well, or recycled (Grady et al., 1995, Iino and Horiguchi 2006).

The receptor for the dominant inhibitory molecule nitric oxide (NO) is intracellular soluble guanylyl cyclase (sGC). Activation of this internal receptor catalyzes the production of cGMP which subsequently activates cGMP dependent kinase PKG which in turn phosphorylates a regulatory protein of calcium activated potassium channels ultimately resulting in hyperpolarization of the cell (Martinet al., 2005, Groneber et al., 2013, Robertson et al 1993). The murine fundus utilizes the binding of NO to sGC in both ICC and smooth muscle for relaxation (Groneberg et al., 2013). The close proximity of neuronal nitric oxide synthase (nNOS) reactive nerves to ICC-DMP, which have strong immunoreactivity for intracellular sGC and PKG, suggest these interstitial cells are prime targets for NO in the relay of inhibitory neurotransmission (Salmhofer et al., 2001).

While there is plenty of evidence suggesting ICC-DMP can respond to excitatory and inhibitory neural stimulation, it is still unclear how ICC-DMP translate these signals and transfer them to nearby smooth muscle cells. Due to the extreme difficulty of recording from ICC-DMP embedded in the circular muscle, it seemed logical to determine how the smooth muscle responds to excitatory neural stimulation of ICC-DMP.

Generally, intracellular recordings from the circular muscle of murine small intestine preparations are paralyzed by nicardipine. If small bowel motor patterns and oscillating populations rely on the fast action of voltage gated calcium channels (namely

the L-type calcium channel), there may be a greater chance of observing the slow low frequency oscillations in the small intestine circular smooth muscle from intracellular recordings in the absence of nicardipine. Without a paralyzing agent the tissue is free to contract, making it impossible to impale and record from a single smooth muscle cell with current microelectrode apparatus. Other authors have bypassed this issue by making tissue preparations much smaller. In many of the following experiments a small preparation (see *2.2.3*) was used where a recording area of exposed circular smooth muscle only 2 by 2 mm excised from surrounding circular muscle. This ensured contractile activity was miniscule (Pluja et al., 2001, Yoneda et al., 2004)

5.2 Methods

Intestinal jejunum segments from adult female CD-1 mice were used for all intracellular recording experiments. Information regarding animal handling and intestinal excision can be found in section 2.1 and 2.2 respectively.

5.2.1 Circular muscle experiments proper

Circular muscle experiments were conducted as described in section *3.2.1*. In all preparations, controls were obtained by recording uninterrupted electrical activity for a period of at least five minutes from a single circular smooth muscle cell. After the control recording, pharmacological agents (100 µM lidocaine or 200 µM L-NNA) were then added to the inflow reservoir of fresh Krebs'' and subsequently perfused on the tissue samples. Ten minutes post addition of 100 µM lidocaine application of 0.5 µM SP was perfused onto the tissue.

5.2.2 Small preparations proper

Tissue was prepared as described in section *2.3.3*. Small preparations were allowed to equilibrate at 37^{o}C one hour prior to experimentation. Small preparation experiments were conducted similarly to circular muscle experiments described in section *3.2.1*. In all preparations, controls were obtained by recording uninterrupted electrical activity for a period of at least five minutes from a single circular smooth muscle cell. After the control recording, pharmacological agents (50 nM SP, 200 µM L-NNA, or both

50 nM SP and 200 µM L-NNA) were then added to the inflow reservoir of fresh Krebs'' and subsequently perfused on the tissue samples.

5.2.3 Data analysis

Raw data was collected and analyzed as described previously in section *3.2.3*.

5.3 Results

When 200 µM L-NNA was perfused onto circular muscle a visually noticeable waxing and waning like electrical pattern in the smooth muscle resolved from a steady slow wave in four of five experiments (Fig 5.2). This pattern is similar to the waxing waning like phenomenon induced by BA on the mucosa intact preparation; the waning wasn't at rhythmic intervals as it was with DA induced waxing waning, and occasionally the slow waves during wanes were greater than 50% of the amplitude of maximally waxing slow waves. The time required to establish this wave pattern varied among preparations (n=4, mean 32.2 ± 3.33 min). Wash out with fresh Krebs'' solution was unable to abolish the waxing waning pattern and restore the original slow wave (n=2).

CWT analysis of the smooth muscle electrical activity during control and reagent stages of the experiment revealed the addition of L-NNA resulted in the onset of the low frequency component. In two cases where the low frequency component was already present during the control recording, the nNOS inhibitor increased the signal the strength of the low frequency component in the smooth muscle (Table 5.1).

The previously mentioned was conducted in the presence of the paralyzing reagent nicardipine. However, in case an aspect of the low frequency component relies on L-type calcium channel activation, the use of nicardipine could be masking an important physiological trait. The small preparations circumvent the issue; preventing muscle contraction without inhibiting calcium entry though the L-type calcium channel.

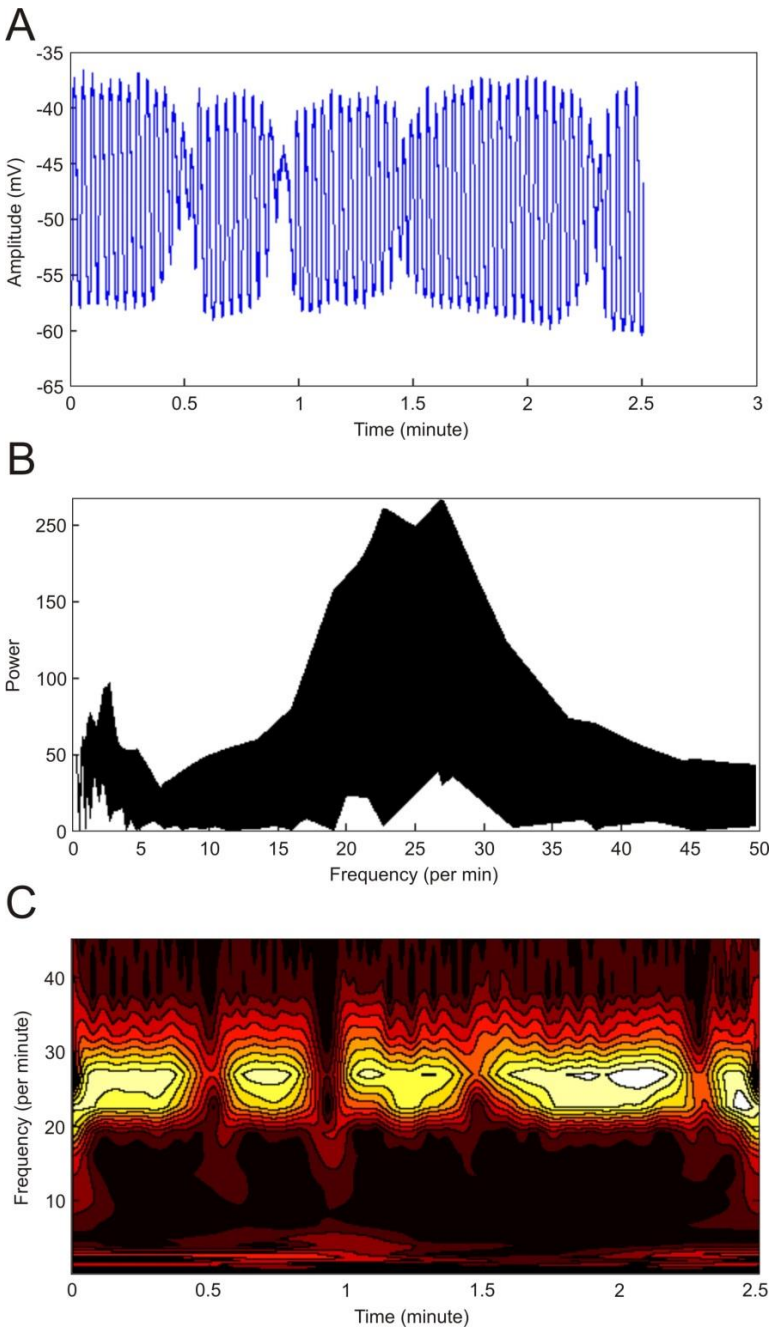

Figure 5.2 Frequency components observed after inhibition of inhibitory neurotransmission. Intracellular electrical activity of circular muscle after addition 200 µM L-NNA (A). Continuous wavelet transformation analysis shows frequency distribution of source (B). Time-frequency contour plot of mean power (continuous wavelet transform analysis) shows a high frequency and a low frequency component (C).

Table 5.1 Analysis of Frequency Components Post 200 µM L-NNA

Experimental stage	N	# Frequency Components	LF (mean)	N(exp)	HF (mean)	N(exp)	HF:LF
Control	14	1.4 ± 0.14	3.0 ± 0.34	6	26.6 ± 0.71	14	3.95 ± 0.62
L-NNA + Nicardipine	5	2.6 ± 0.40	3.2 ± 0.51	5	26.2 ± 0.49	5	3.0 ± 0.42
Small Prep	4	2 ± 0.0	2.69 ± 0.28	4	25.0 ± 1.68	4	2.66 ± 0.16
Small Prep + Nicardipine	5	1.8 ± 0.2	4.62 ± 0.52	4	27.36 ± 1.20	5	1.77 ± 0.30

(DA) Decanoic acid, (LF) low frequency, (HF) high frequency
Frequency components refers to how many frequency components isolated
N(exp) states how many experiments of total N displayed previous frequency component

Interestingly, L-NNA applied to the small preparations did not result in the visually obvious waxing waning like pattern (n=4; Fig 5.3A). Generally it was extremely difficult to determine if there was any increased low frequency activity. Due to the difficulty in observing visible changes in the electrical patterns CWT analysis was performed on recordings approximately 38 minutes after the addition of L-NNA to the inflow reservoir, unless an otherwise obvious change was observed. Thirty eight minutes was determined because in the previous experiment it required approximately 32 minutes for the waxing waning like phenomenon to occur post 200 μM L-NNA. The extra six minutes were to allow stabilization of the pattern and ensure the upper range (later onset) could be analyzed. CWT analysis identified the presence of a low frequency component with an HF:LF ratio less than three after the addition of L-NNA in every experiment (n=4, mean HF:LF = 2.66 ± 0.16; Table 5.1, Fig 5.3B, C). In two of four experiments the low frequency component was present before the addition of L-NNA, but had a HF:LF ratio above three indicating it was too weak to influence the slow wave patter. L-NNA increased the relative power of the low frequency component to the high frequency component in both experiments.

Perhaps the presence of nicardipine was the reason the influence of the low frequency component was hardly observed. When L-NNA was added to standard circular muscle tissue preparations paralyzed by nicardipine visual waxing waning was observed (Fig 5.2). When perfused onto small preparations without nicardipine the low frequency component was induced, but waxing waning never arose (Fig 5.3). Thus, to reduce the number of uncontrolled variables from two to one, the small preparations were paralyzed

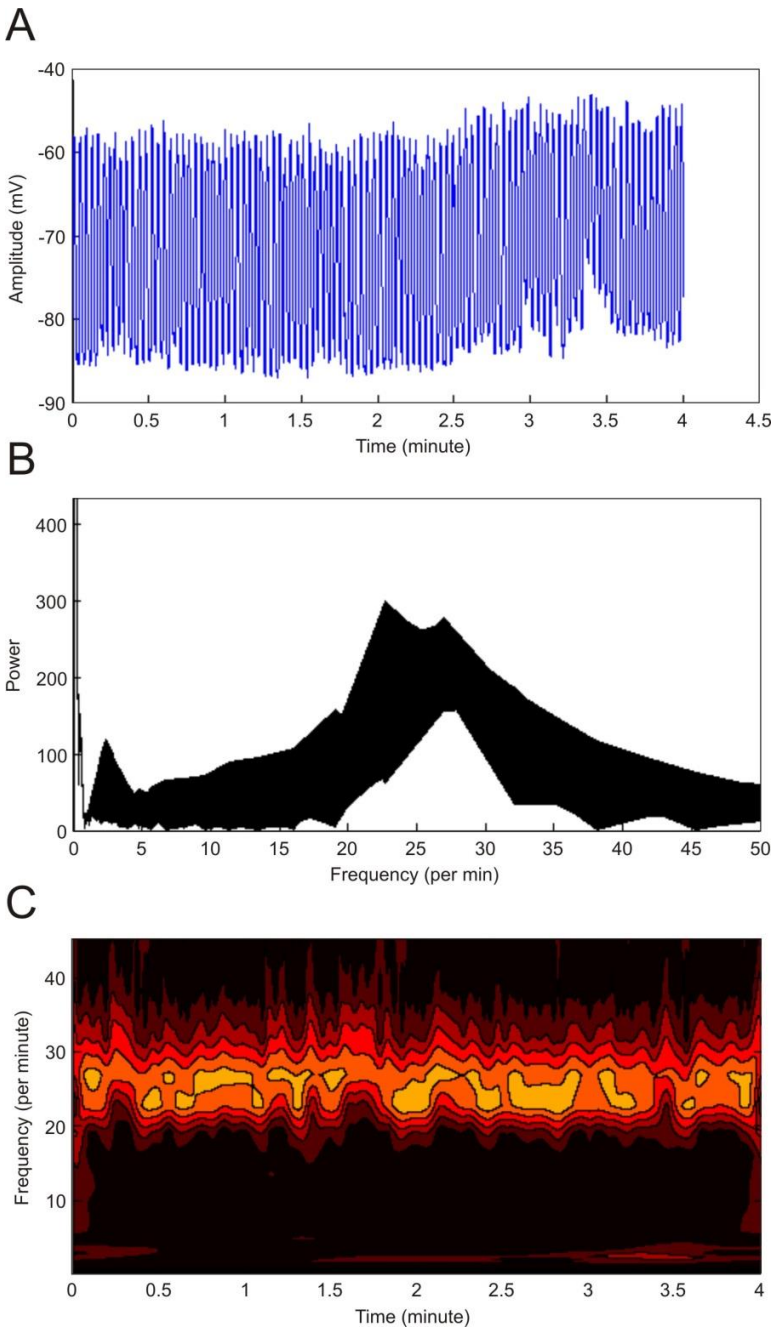

Figure 5.3 Frequency components observed after inhibition of inhibitory neurotransmission on small preparations. Intracellular electrical activity of circular muscle after addition 200 µM L-NNA (A). Continuous wavelet transformation analysis shows frequency distribution of source (B). Time-frequency contour plot of mean power (continuous wavelet transform analysis) shows a high frequency and a low frequency component (C).

with 0.5 µM nicardipine prior to the experiment. Like prior L-NNA experiments, addition of the nNOS inhibitor induced the onset of low frequency component. In three of five experiments a waxing waning like pattern could be observed during perfusion of 200 µM L-NNA, similar to that shown in Figure 5.2. This demonstrated the presence of nicardipine may be required to observe the low frequency component.

The use of small preps was useful in preventing contractions when excitatory neurotransmitters were applied to the tissue. Addition of 50 nM SP to the small tissue preparations did not result in any significant change to the electrical pattern displayed by the circular smooth muscle cells within forty minutes. Although not visually obvious, in two of four experiments CWT analysis indicated a low frequency component was introduced, however the HF:LF ratio was too large (n=4, mean 3.9 ± 0.74) suggesting and underwhelming presence (Table 5.2). In experiments where a low frequency component was present during control recordings, SP did not increase the power.

In an attempt to further excite ICC-DMP, 200 µM L-NNA and 50 nM SP were both perfused simultaneously onto tissue preparations. Interestingly, in two of five experiments, while not inducing an obvious rhythmic waxing waning pattern, CWT analysis revealed addition of the nNOS inhibitor and the tachykinergic neurotransmitter stimulated the onset of a low frequency component, however the HF:LF ratio was greater than three (Table 5.2). In the remaining three of five experiments the effects of both reagents were hardly noticeable after forty minutes of recording post addition.

Table 5.2 Analysis of Frequency Components on Small Preparations

Experimental step	N	# Frequency Components	LF (mean)	N(exp)	HF (mean)	N(exp)	HF:LF
Control	9	1.67 ± 0.17	4.2 ± 1.01	5	24.2 ± 1.20	9	3.62 ± 0.29
SP	4	2 ± 0.0	2.62 ± 0.52	4	26.2 ± 1.49	4	3.9 ± 0.74
L-NNA SP	5	1.8 ± 0.2	4.0 ± 0.41	4	20.6 ± 0.98	5	3.3 ± 0.33

(L-NNA) Nω-Nitro-L-Arginine, (SP) Substance P, (LF) low frequency, (HF) high frequency
Frequency components refers to how many frequency components isolated
N(exp) states how many experiments of total N displayed previous frequency component

In attempt to record the effects of SP without neural involvement, 100 µM lidocaine was used to prevent excitation (action potential activity) of tachykinergic nerves, and subsequent neural network signaling. Standard circular muscle preparations (see *3.2.1*) paralyzed with 1 µM nicardipine were utilized. In control experiments 100 µM lidocaine was added after a control recording was obtained. The voltage gated sodium channel blocker did not induce low frequency activity after 40 minutes of perfusion (n=3). The control determined lidocaine was not a low frequency component stimulant. To determine if SP can influence smooth muscle activity without neural involvement, 0.5 µM SP was added to the inflow reservoir after tissue had been exposed to lidocaine for duration of 10 minutes. Perfusion of the tachykinergic neurotransmitter induced the onset of the low frequency component (n=4, mean 3.62 ± 0.55) and waxing waning pattern (Table 5.3, Fig 5.4). The time required to induce the waxing waning like phenomenon varied among preparations (n=4, mean 22.2 ± 2.95 min).

Table 5.3 Analysis of Frequency Components Post Neural Blockade

Experimental stage	N	# Frequency Components	LF (mean)	N(exp)	HF (mean)	N(exp)	HF:LF
Control	6	1.83 ± 0.17	3.9 ± 0.24	5	31.7 ± 1.67	6	3.9 ± 0.40
Lidocaine	6	1.33 ± 0.21	3.0 ± 1.0	2	31.0 ± 1.37	6	3.5 ± 0.80
SP	4	1.75 ± 0.25	3.62 ± 0.55	4	29.5 ± 1.44	4	1.90 ± 0.41

(SP) Substance P, (LF) low frequency, (HF) high frequency
Frequency components refers to how many frequency components isolated
N(exp) states how many experiments of total N displayed previous frequency component

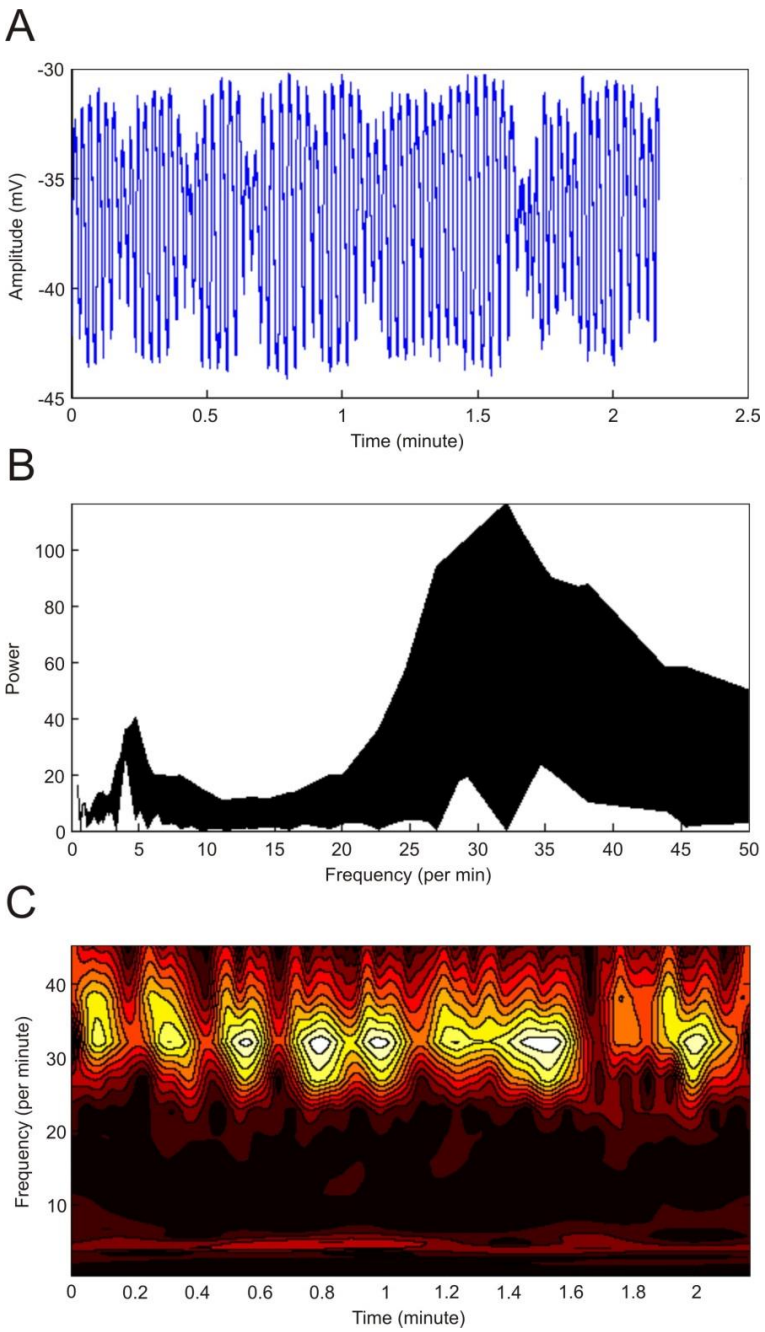

Figure 5.4 Frequency components observed after addition of substance P onto lidocaine treated tissue. Intracellular electrical activity of circular muscle after addition of 0.5 µM SP (A). Continuous wavelet transformation analysis shows frequency distribution of source (B). Time-frequency contour plot of mean power (continuous wavelet transform analysis) shows a high frequency and a low frequency component (C).

5.4 Discussion

In the presence of nicardipine the circular smooth muscle cells responded to the addition of 200 µM L-NNA. A waxing waning like pattern similar to that induced by BA emerged (see *3.3.2*). Inhibition of nNOS prevents the production of nitric oxide, the diffusible inhibitory neurotransmitter. While smooth muscle cells have been shown to express the intracellular receptor sGC and can respond to NO stimulation (Groneberg et al., 2013) it is unlikely they themselves are responsible for producing a low frequency oscillation when NO mediated inhibition is abolished. There is a much more likely reason the low frequency component arose. Parallel to the LFHA oscillations of the murine colon, activity of the ICC-DMP (which expresses cytosolic sGC) may be under tonic inhibition by NO. The low frequency component could be suppressed and alleviation of this inhibition would thereby be a possible mechanism for its increased activity. The response time (mean 32.2 + 3.33 min) was expected as substantial time is required to inhibit nNOS activity from producing further NO, and breakdown of existing NO in the system.

Interestingly, with the small preparation, addition of the same concentration of L-NNA, in the absence of nicardipine, did not induce the obvious waxing waning pattern observed in the prior experiment. Unless for the CWT analysis of the voltage time recordings, it would have been almost impossible to determine the low frequency component was induced in two experiments. Perhaps the fast flow of calcium through the L-type calcium channel prevented observation of the slowly depolarizing low frequency

signal transduction into the smooth muscle; thus the waxing waning phenomenon was not observed. Another possibility lies within the flaw of the preparation design. The small preparations (2 by 2 mm) may be too small, and excising the surrounding tissue (see *2.2.3*) may have physically disrupted the existing networks preventing phase amplitude coupling. This speculation assumes a substantial size of tissue, perhaps even larger than standard circular muscle preparations (see *2.2.1*), and thus connected cells are required to effectively propagate the low frequency signal into the musculature.

Summarized, in the presence of nicardipine L-NNA was able to induce waxing waning, and without the L-type calcium channel blocker it was not. It seemed as though either the presence of nicardipine or the limitations of the small preparation influences whether or not L-NNA will induce the waxing waning phenomenon. To test if the L-type calcium channel plays a role in observing the waxing waning phenomenon L-NNA was added to small preparations paralyzed with nicardipine. While the low frequency component was induced in all samples, the waxing waning like pattern emerged in three of five experiments. This would suggest blockage of the L-type calcium channel is required to observe the waxing waning phenomenon. However, because waxing waning was not observed in all experiments, the limitations of the small preparation in terms of consistency become evident. Careful interpretation of results for all small preparation experiments becomes apparent.

Addition of 50 nM SP to the small preparation failed to alter any parameter of slow wave pattern, or introduce a low frequency component of any significant power (HF:LF > 3.0). This was a strange result; it is known that ICC-DMP express NK1r, the SP

receptor, thus addition of the neurotransmitter should have stimulated ICC-DMP activity and thus onset of the low frequency component. Although the faults of the preparation must be taken into consideration, even if no change to the slow wave pattern was observed, if SP could activate low frequency activity it would be apparent after CWT analysis; which it was not. There are three possible reasons outlined which may have causes SP to fail in inducing a response: i) ICC-DMP stimulation by SP is unable to produce the low frequency component because it is under tonic inhibition from NO; ii) SP has different effects on excitatory motor nerves and on ICC-DMP, such that SP stimulation of motor neurons counteracts the effect SP has on ICC-DMP; or iii) the concentration of SP is too small. In the second scenario (ii) ICC-DMP may be stimulated by SP, but unable to influence the adjacent smooth muscle.

Addressing the first point (i), 200 µM L-NNA and 50 nM SP were simultaneously added to co-influence the smooth muscle small preparation via the ICC-DMP. The nNOS inhibiter and neurotransmitter induced the low frequency component in two of five experiments, but had no effect in the remaining three. This result is very difficult to interpret, as it is not conclusive, however co-stimulation cannot be ruled out. It would seem in certain experimental conditions abolishment of NO mediated inhibition and tachykinin stimulation can induce the low frequency component and produce waxing waning. It also demonstrates some unknown variable can prevent the phenomenon from occurring at all. There seem to be many flaws with this experiment. Addition of L-NNA to small preparations always resulted in the onset of a low frequency component. However, with co-stimulation the low frequency component was only introduced in two

of five experiments, and when it was observed, the HF:LF ratio was too large (HF:LF > 3) indicating a non-influential presence. L-NNA requires a substantial amount of time (mean 32.2 + 3.33 min) to exert its effect. SP on the other hand is generally a fast acting neurotransmitter. Since neural activity was not inhibited, SP could have produced an excitatory effect on excitatory motor neurons which in turn could have prevent the later effects of L-NNA from occurring. It seemed necessary to abolish neural activity.

In regards to the third plausible reason 50 nM SP failed to induce a response (iii), Kim et al. (2012), required 0.5 µM SP to alter pacemaking activity in cultured ICC clusters. On a standard circular muscle preparation paralyzed with nicardipine, lidocaine was utilized to abolish neural activity. A high concentration of SP (0.5 µM) induced the low frequency component and produced the waxing waning phenomenon. Without a neural response to SP it is likely the neurotransmitter solely stimulated ICC-DMP activity.

ICC-DMP networks of the small intestine are clearly influenced by inhibitory and excitatory enteric neurotransmission. The population of ICC-DMP seem to be under a tonic inhibitory control, which when released allow the pseudo pacemaker cells to produce the low frequency signal. Additionally, ICC-DMP are receptive to excitatory tachykinergic neurotransmission and can produce low frequency oscillations in response to excitation.

6. GENERAL DISCUSSION

6.1 Summary of findings

The focus of my research has been on investigation of the segmentation motor pattern of the mouse small intestine at the cellular level, identifying key participatory cells and their contribution. Studies of change in electrical activity of individual circular smooth muscle cells were imperative to understanding the influence of rhythmic oscillators present in the gastrointestinal tract.

I have shown the waxing waning phenomenon is an inducible pattern that responds to identical stimulus which induces segmentation. Emergence of a secondary slowly oscillating low frequency pacemaker, based on my research, is responsible for the alteration of regular slow wave activity into the waxing waning pattern, which I believe parallels segmentation. The medium chain fatty acid, decanoic acid, perfused onto the circular muscle initiated the low frequency oscillations which ultimately produced waxing waning in the presence of neural blockade. The short chain fatty acid, butyric acid, also invoked the waxing waning phenomenon when applied the mucosa of the small intestine jejunum. Thus, this low frequency component can be initiated by both myogenic and neural means. The rhythmicity associated with both DA and BA induced waxing waning points to a myogenic origin of rhythmicity.

Previously, the slow wave generating ICC-MP were the only known and well investigated pacemaker cells. Abolition of the high frequency slow wave through

destruction of ICC-MP networks did not alter the capabilities of the low frequency oscillator, indicating the signal is not produced by the dominant ICC-MP populations. ICC-DMP, unaltered in W^v mice and unaffected by methylene blue mediated ICC-MP mitochondrial disruption, became a prime candidate for the low frequency oscillator. ICC-DMP responded to alleviation of inhibitory control via nitric oxide and to excitatory tachykinergic neurotransmission, both of which resulted in production of a low frequency signal and the associated onset of the waxing waning phenomenon.

Piecing the story together from the evidence provided in this thesis, the ICC-DMP networks of the murine small intestine are responsible for the stimulated generation and transmission of the low frequency low amplitude oscillation into the adjacent circular smooth muscle cells. Stimulants of ICC-DMP activity currently known as of this study are: decanoic acid, butyric acid, and substance P. Nitric oxide plays an inhibitory role silencing the ICC-DMP. Within the muscularis, the ICC-DMP low frequency depolarization and the high frequency slow wave of the ICC-MP clearly interact, likely through phase-amplitude coupling, to produce the waxing waning phenomenon. Waxing and waning is likely the cellular electrical activity smooth muscle cells experience when involved in whole organ segmentation contractions.

The studies performed over the duration of my thesis focused on the waxing waning phenomenon in individual circular smooth cells, and the interaction between pacemaker systems. It is inherently clear, through my research and thorough assessment of the literature, the interactions between myogenic and neurogenic control systems are required to wholly comprehend all gastrointestinal motor patterns. Investigation into the

mechanisms inducing dominant gastrointestinal motor patterns is crucial for drug development; more research will discover additional targets capable of altering motor activity.

6.2 Diagrammatic Model of Findings

The findings of this thesis are incredibly important in the study of the segmentation motor pattern; suggesting a novel mechanism of initiation involving distinct pacemaker populations (Fig 6.1).

The medium chain fatty acid, decanoic acid, shown to induce the segmentation motor pattern (Gwynne et al., 2004) induced the waxing waning phenomenon of circular muscle electrical activity in the mouse small intestine. The waxing waning electrical pattern was inspected with continuous wavelet transformation analysis to distinguish frequency components involved in the generation of the signal. A high frequency component (at the characteristic frequency of the slow wave) and a low frequency component were consistently isolated from waxing waning recordings.

It was speculated the waxing waning phenomenon could be reproduced by phase-amplitude coupling of the low and high frequency oscillations respectively. In this sense, the phase of the low amplitude low frequency oscillations modified the amplitude of the high frequency slow wave.

The low frequency component could be stimulated by the medium chain fatty acid, decanoic acid, and the short chain fatty acid, butyric acid. Additionally, the same

neurotransmitters we would expect to influence the ICC-DMP affected the low frequency component. ICC-DMP are co-localized with nNOS containing neurons (Wang et al. 2003), and were determined to be under tonic inhibition by nitric oxide. Inhibition of this inhibition produced the low frequency component and waxing waning of slow wave activity. Additionally, ICC-DMP express numerous receptors for the tachykinergic excitatory neurotransmitter substance P (Faussone-Pellegrini 2006). Substance P was shown to stimulate the low frequency oscillator and the waxing waning phenomenon.

In conclusion I determined a low frequency oscillator, stimulated by neurotransmission and fatty acids, interacts with the high frequency slow wave component in the circular smooth muscle to produce the waxing waning phenomenon correlated to segmentation

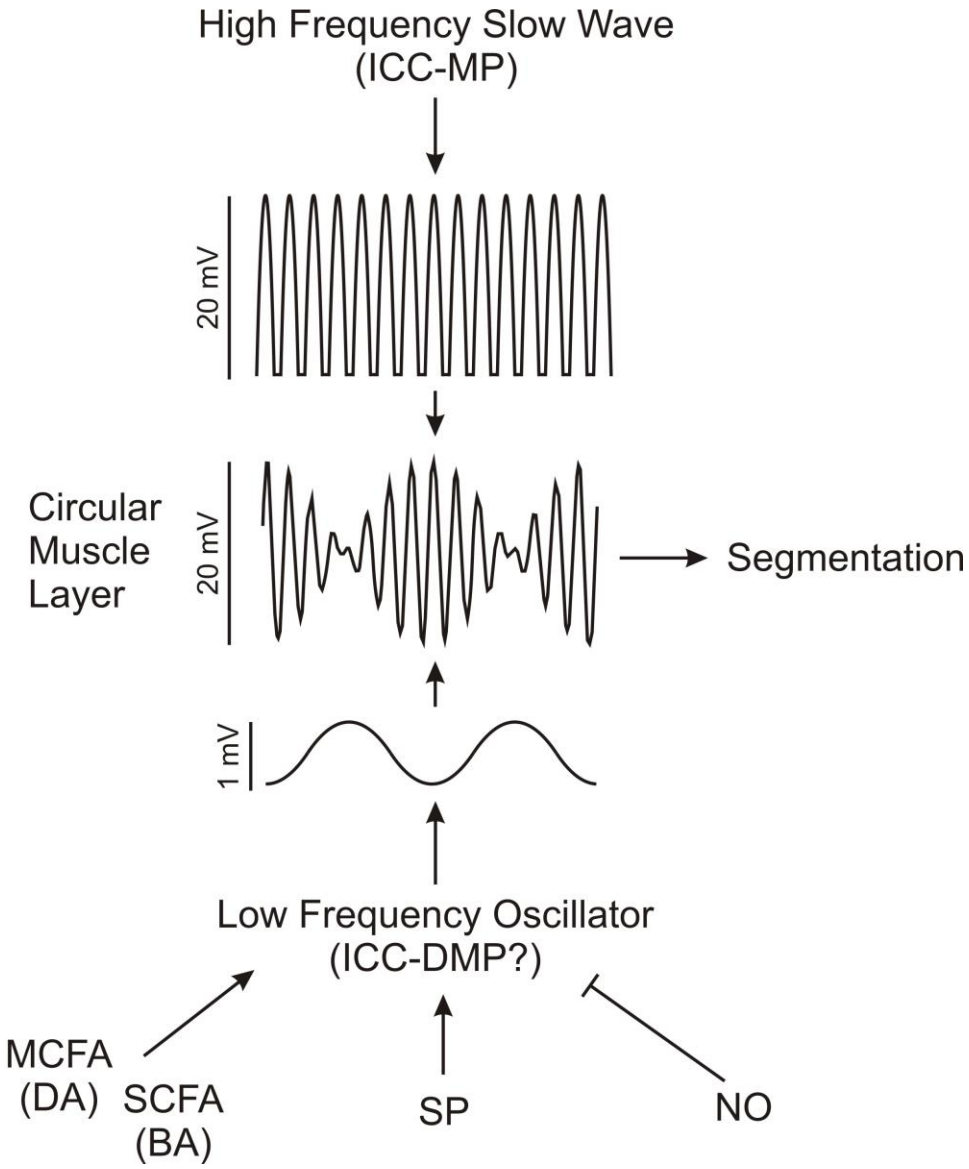

Figure 6.1 Schematic diagram of findings. The segmentation motor pattern exhibited by the small intestine to facilitate mixing and absorption of content can be initiated by the onset of the waxing waning phenomenon. Waxing and waning of slow wave amplitude is achieved by phase-amplitude coupling between low frequency oscillations and high frequency ICC-MP activity respectively. The low frequency oscillator, suspected to be the ICC-DMP networks, is stimulated by luminal nutrients including decanoic acid (DA) and butyric acid (BA); by tachykinergic excitatory neurotransmission (substance P, SP); and is under tonic inhibition by nitric oxide (NO).

6.3 Experimental limitations

Ultimately, *in vivo* research provides the most accurate data in regards to motility studies. Although obtaining date from small paralyzed micro-dissected tissue samples kept alive in baths of isotonic salt solution is convenient, it is far off from replicating physiological conditions as they would exist *in vivo*. The miniscule size of small preparations may have severed crucial ICC network connections and communicating neural processes, which could have led to an incomplete understanding of the results obtained.

Recording electrical voltage activity from a single cell had additional limitations. Over time the cellular membrane seal around the microelectrode degrades resulting in leakage of cytoplasmic fluids. Subsequently electrical recordings would accumulate more noise before cell death. Movement of the tissue accelerated this effect. The hemi-dissected tissue preparation increased the difficulty of successfully recording from muscle cells. The preparation required two separate inflows to perfuse control Krebs' and reagent simultaneously at the same rate. However, due to equipment limitations, the inflow rates were slightly different, and this in turn prevented continuous outflow. Loss of continuous outflow was associated with a substantial increase in noise and movement of the microelectrode which precluded many successful recordings.

Specific to the W^v small intestine circular muscle, recording intracellular electrical activity was extremely difficult as the W^v lack distinguishable baseline activity.

Recording small electrical fluctuations from the bath medium was often mistaken for successfully penetrating and observing smooth muscle cells.

Throughout the research presented in this thesis, all intracellular recordings were of the circular smooth muscle layer. Ideally, to ensure the ICC-DMP networks are in fact responsible for the low frequency oscillation, recording directly from these interstitial cells would have provided more convincing data. Unfortunately, these networks are embedded within the smooth muscle layer and most reliable methods to isolate the ICC-DMP are too invasive, often resulting in destruction of the outer circular muscle division with no way to ensure ICC-DMP integrity until post experimentation.

While the continuous wavelet transformation may be the best algorithm for isolating variable frequency components over a specific time frame, there are inherent issues which need to be discussed. The major issue comes from the uncertainty principle, originally formulated by Heisenberg, which states both the momentum and position of a moving particle cannot be known simultaneously. In regards to determining frequency components over time, the frequency and time information of a signal cannot be pinpointed in the time-frequency plane. This is a problem of resolution; high frequencies are better resolved in time, while lower frequencies are better resolved in frequency. Thus, a high frequency component can be better located in time than a low frequency component. Due to the uncertainty principle and the trade-off in resolution, the CWT analysis performed throughout the work of this thesis may not provide justice to the relative strength of frequency (power spectrum) between the high and low frequency components.

6.4 Future Experiments

The primary technique utilized in the work of this thesis was the intracellular recording technique. While this method provides insight to the activity induced by pharmacological agents and nutrients at the cellular level, it does not reveal how these reagents affect the organ as a whole. Spatio-temporal mapping of whole organ contractile activity is an excellent method to observe the end result on motility of interacting pacemaker activity in a system close to *in vivo* settings. Similar to the circular muscle (see 3.*2.1*) and hemi-dissected mucosa intact preparations (see 3.*2.2*), nutrients could be applied to the mouse small intestine in bath solution or injected through intra-luminal means respectively. This would provide key information as to how the waxing waning phenomenon of single smooth muscle cell activity is related to whole organ contractile activity. The organ bath would not be limited to just the use of nutrient reagents; the effects of substance P and L-NNA on quiescent tissue could allow the observation of the onset of the low frequency component in the correct conditions.

Low frequency isolation through abolishment of ICC-MP activity could be applied to the whole organ bath technique. While results from the W^v mouse have been unfruitful in observing the on/off capabilities of ICC-DMP activity, perhaps the methylene blue mediated ICC-MP mitochondrial destruction procedure could be modified for whole organ preparations. If the high frequency activity of the ICC-MP could be annihilated, perhaps in the presence of neural blockade decanoic acid or substance P could be utilized to see if low frequency contractions emerge.

The focus of future experiments thus far has been on organ bath motility studies. While this is necessary to understand how the low frequency component influences small intestines motor patterns, comprehension of the propagation of the low frequency oscillations into the smooth muscle is required to understand how it produces the waxing waning phenomenon in the circular smooth muscle layer. This could be achieved by cross sectional studies of the circular muscle layer. Two microelectrodes could record electrical activity from different points of the muscle thickness: one could penetrate the middle of the circular muscle layer, and the other could record electrical activity from circular muscle adjacent to ICC-DMP networks. This procedure could determine the active (regenerative) or passive (gradually decaying) nature of the low frequency oscillation through the musculature. It could also reveal how the low frequency and high frequency interactions vary throughout the muscle thickness.

REFERENCES

Ailiani AC, Neuberger T, Brasseur JG, Banco G, Wang Y, Smith NB, Webb AG (2009) Quantitative analysis of peristaltic and segmental motion in vivo in the rat small intestine using Dynamic MRI. *Magn Reson Med* **62**: 116-126.

Alexandre H, Mathieu B, Charpentier C (1996) Alteration in membrane fluidity and lipid composition, and modulation of H -ATPase activity in Saccharomyces cerevisiae caused by decanoic acid. *Microbiol* **142**: 469-475.

Beck TW, Housh TJ, Johnson GO, Cramer JT, Weir JP, Coburn JW, Malek MH (2006) Comparison of the fast fourier transformation and continuous wavelet transformation for examining mechanomyographic frequency versus eccentric torque relationships. *J Neurosci Methods* **150**: 59-66.

Belluscio MA, Mizuseki K, Schmidt R, Kempter R, Buzaki G (2002) Cross-Frequency Phase-Phase coupling between Theta and Gamma oscillations in the Hippocampus. J. Neurosci **32**: 423-435.

Benabdallah H, Messaoudi D, and Gharzouli K (2008) The spontaneous mechanical activity of the circular smooth muscle of the rabbit colon in vitro. *Pharmacol Res* **57**: 132-141.

Bortoff A (1965) Electrical transmission of slow waves from longitudinal and to circular intestinal muscle. *Am J Physiol* **209**: 1254-1260.

Brown NJ, Read NW, Richardson A, Rumsey RDE, Bogentoft (1990) Characteristics of lipid substances activating the ileal brake in the rat. *Gut*. 1990 **31**: 1126-1129.

Bueno L, Fioramonti J, Ruckebusch Y, Frexinos J, and Coulom P (1980) Evaluation of colonic myoelectrical activity in health and functional disorders. *Gut* **21**: 480-485.

Burt JM, Massey KD, Minnich BN (1991) Uncoupling of cardiac cells by fatty acids: structure-activity relationships. *Am J Physiol Cell Physiol* **260**: C439-C448.

Cannon WB (1902) The movements of the intestine studied by means of the Röntgen rays. 1902 *Am J Physiol* **107**:641-664.

Cano-Cebrian MJ, Zornoza T. Granero L Polache A (2005) Intestinal absorption enhancement via the paracellular route by fatty acids chitosans and other: a target for drug delivery. *Curr Drug Delivery* **2**: 9-22.

Costa M, Brookes SJH, and Hennig GW (2000) Anatomy and physiology of the enteric nervous system. *Gut* **47**: iv15-iv19.

De Backer O, Elinck E, Priem E, Leybaert L, Lefebvre RA (2009) Peroxisome proliferator-activated receptor γ activation alleviates postoperative lleus in mice by inhibition of Egr-1 expression and its downstream target genes. *J Pharmacol Exp Ther* **331**: 496-503.

Der-Silaphet T, Malysz J, Hagel S, Arsenault AL, Huizinga JD (1998) Interstitial cells of Cajal direct normal propulsive contractile activity in the mouse small intestine. *Gastroenterology* **114**: 724-736.

Diamant NE and Bortoff A (1969) Nature of the intestinal low-wave frequency gradient. *Am J Physiol Legacy Content* **216**: 301-307.

Dickson EJ, Heredia DJ, McCann, CJ, Hennig GW, and Smith TK (2010) The mechansims underlying the generation of the colonic migrating motor complex in both wild-type and nNOS knockout mice. *Am J Physiol Gastrointest Liver Physiol* **298**: G222-G232.

Diener M, Vujicic Z, Scharrer E (1996) Neuronally mediated anion secretion induced by short chain fatty acids in the rat distal small intestine. *Acta Physiol Scand* **157**: 33-40.

Donnelly G, Jackson TD, Ambrous K, Ye J, Safdar A, Farraway L, Huizinga JD (2001) The myogenic component in distention-induced peristalsis in the guinea pig small intestine. *Am J Physiol Gastrointest Liver Physiol* **280**: G491-500.

Faussone-Pellegrini MS (2006) Relationships between neurokinin receptor-expressing interstitial cells of Cajal and tachykininergic nerves in the gut. *J Cell Mol Med* **10**: 20-32.

Garcia-Lopez P, Garcia-Marin V, Martinez-Murillo R, Freire M (2009) Updating old ideas and recent advances regarding the Interstitial Cells of Cajal. *Brain Res Rev* **61**: 154-169.

Grady EF, Garland AM, Gamp PD, Lovett M, Payan DG, and Bunnett NW (1995) Delineation of the Endocytic Pathways of Substance P and its seven-transmembrane domain NK1r receptor. *Mol Biol Cell* **6**: 509-524.

Groneberg D, Lies M, Konig P, Jager R, Seidler B, Klein S, Saur D, Friebe A (2013) Cell-specific deletion of nitric oxide sensitive guanylyl cyclase reveals a dual pathway for nitrergic neuromuscular transmission in the murine fundus nitrergic relaxation in nitric oxide sensitive guanylyl cyclase knockout mice. *Gastroenterology* **145:** 188-196.

Guilloteau P, Martin L, Eeckhaut V, Ducatelle R, Zabielski R, Immerseel FV (2010) From the gut to the peripheral tissues: the multiple effects of butyrate. *Nutr Res Rev* **23**: 366-384.

Gwynne RM, Thomas E, Goh S, Sjövall H, Bornstein J (2004) Segmentation induced by intraluminal fatty acid in isolated guinea-pig duodenum and jejunum. *J Physiol* **556**: 557-569.

Gwynne RM and Bornstein JC (2007) Mechanisms underlying nutrient-induced segmentation in isolated guinea pig small intestine. *Am J Physiol Gastrointest Liver Physiol* **292**: G1162-G1172.

Hirschi KK, Minnich BN, Moore LK, Burt JM (1993) Oleic acid differentially affects gap junction-mediated communication in heart and vascular smooth muscle cells. *Am J Physiol Cell Physiol* **265**: C1517-C1526.

Hou X, Yin J, Liu J, Paericha PJ, and Chen JDZ (2005) In vivo gastric and intestinal slow waves in W/Wv mice. *Dig Dis Sci* **50**: 1335-1341.

Huber A, Trudrung P, Storr M, Franck H, Schusdziarra V, Ruth P, and Allescher HD (1998) Protein kinase F expression in the small intestine and functional importance for smooth muscle relaxation. *Am J Physiol Gastrointest Liver Physiol* **275**: G629-G637.

Hudson N, Mayhew I, Pearson G (2002) Presence of in vitro electrical activity in the ileum of horses with enteric nervous system pathology: equine dysautonomia (grass sickness). *Auton Neurosci* **99**: 119-126.

Hudson N, Mayhew I, Pearson G (2006) Interstitial cells of Cajal and electrical activity of smooth muscle in porcine ileum. *Acta Physiologica* **187**: 391-397.

Huizinga J, Liu L, Blennerhassett M, Thuneberg L, Molleman A (1992) Intercellular communication in smooth muscle. *Cell Mol Life Sci* **48**: 932-941.

Huizinga JD, Thuneberg L, Kluppel M, Malysz J, Mikkelsen HB, and Berstein A (1995) W/kit gene required for interstitial cells of Cajal and for intestinal pacemaker activity. *Nature* **373**: 347-340.

Huizinga JD, Thuneberg L, Vanderwinder JM, and Rumessen JJ (1997) Interstitial cells of Cajal as targets for pharmacological intervention in gastrointestinal motor disorders. *Trends Parmacol Sci* **18**: 393-403.

Huizinga JD, Ambrous K, Der-Silaphet T (1999) Co-operation between neural and myogenic mechanisms in the control of distension-induced peristalsis in the mouse small intestine. *J Physiol* **506**: 843-856

Huizinga JD, Chen J, Zhu YF, Pawelka AJ, McGinn R, Parsons S, Kunze W, Wu R, Bardakjian B, Ma J, Khosdel A, Hu X, Chen S, Yin S, Zhang Q, Gao Q, Li K, Yu Y, Pistilli M, Collins P, Zarate N, Bercik P, Zhang R, and Chen D (2013) The origin of the segmentation motor activity in the intestine. In review, submitted August 2013 to *Nature Commun*.

Iino S and Horiguchi K (2006) Interstitial cells of cajal are involved in neurotransmission in the gastrointestinal tract. *Acta Histochem Cytochem* **39:** 145-153.

Jimenez M, Cayabyab F, Vergara P, Daniel E (1996) Heterogeneity in electrical activity of the canine ileal circular muscle: interaction of two pacemakers. *Neurogastroenterol Motil* **8**: 339-349.

Kato T, Nakamura E, Imaeda K, and Suzuki H (2009) Modulation of the activity of two pacemakers by transmural nerve stimulation in circular smooth muscle preparations isolated from the rat proximal colon. *J. Smooth Muscle Res* **45**: 249-268.

Kazuhide Horguchi, and Komuro Terumasa (2000) Ultrastructural observations of fibroblast-like cells forming gap junctions in the W/Wv mouse small intestine. J. Autonomic. *Nerv Syst* **80**: 142-147.

Kim BJ, Chang IY, Choi S, Jun JK, Jeon JH, Xu WX, Kwon YK, Ren D, and So I (2012) Involvement of Na+-leak channel in substance P – induced depolarization of pacemaking activity in interstitial cells of Cajal. *Cell Physiol Biochem* **29**: 501-510.

Kirkwood KS, Bunnett NW, Maa J, Castagliolo I, Liu B, Gerard N, Zacks J, Pothoulakis C, Grady EF. D (2001) Deletion of neutral endopeptidase exacerbates intestinal inflammation induced by *Clostridium difficile* toxin A. *Am J Physiol Gastroinest Liver Physiol* **281**: G544-G551.

Kito Y and Suzuki H (2003) Properties of pacemaker potentials recorded from myenteric interstitial cells of Cajal distributed in the mouse small intestine. *J Physiol* **553**: 803-818.

Kito Y, Ward SM, and Sanders KM (2005) Pacemaker potentials generated by interstitial cells of Cajal in the murine intestine. *Am J Physiol Cell Physiol* **288**: C710-C720.

Martin E, BerkaV, Tsai AL, and Murad F (2005) Soluble Guanylyl cyclase: the nitric oxide receptor. *Methods Enzymol* **396**: 478-492.

Komuro T (2006) Structure and organization of interstitial cells of Cajal in the gastrointestinal tract. *J Physiol* **576**: 653-658.

Kleszczyński K and Składanowski AC (2009) Mechanism of cytotoxic action of perfluorinated acids.: I. Alteration in plasma membrane potential and intracellular pH level. *Toxicol Appl Pharmacol* **234**: 300-305.

Kunze WA (1998) A mobile intracellular microelectrode designed to record from neurons in contracting tissue. *Brain Res Protocols* **3**: 94-99.

Kunze WA, Mao YK, Wand B, Huizinga JD, Ma X, Forsythe P, Bienenstock J (2009) Lactobacillus reuteri enhances excitability of colonic AH neurons by inibiting calcium-depending potassium channel opening. *J Cell Mol Med* **13**: 2261-2270.

Kurahashi M, Niwa Y, Cheng J, Ohsaki Y, Fujita A, Goto H, Fujimoto T, and Torihashi S (2008) Platelet-derived growth factor signals play critical roles in differentiation of longitudinal smooth muscle cells in mouse embryonic gut. *Neurogastroenterol Motil* **20**: 521-531.

Lee SE, Wi JS, Min YI, Jung C, Ahn KY, Bae CS, Kim BY, Park SS, Oh CS, Weninger WJ, and Nam KI (2009) Distribution and three dimensional appearance of the interstitial cells of Cajal in the rat stomach and duodenum. *Microsc Res Tech* **72**: 951-956.

Lees-Green R, Du P, O'Grady G, Beyder A, Farrugia G, and Pullan AJ (2011) Biophysically based modeling of the interstitial cells of Cajal: current status and future perspectives. *Front Physiol* 2:29 **doi**: 10.3389/fphys.2011.00029.

Legras J, Erny C, Le Jeune C, Lollier M, Adolphe Y, Demuyter C, Delobel P, Blondin B, and Karst F (2010) Activation of two different resistance mechanisms in Saccharomyces cerevisiae upon exposure to octanoic and decanoic acids. *Appl Environ Microbiol* **76**: 7526-7535.

Lindmark T, Kimura Y, and Artursson P (1998) Absroption enhancement through intracelluler regulation of tight junction permeability by medium chain fatty acids in Caco-2 Cells. *J Pharm Exp Therap* **284**: 362-369.

Liu LWC and Huizinga JD (1993) Electrical coupling of circular muscle to longitudinal muscle and interstitial cells of Cajal in the canine colon. *J Physiol* **470**: 445-461.

Liu L, Thuneberg L, and Huizinga JD (1994) Selective lesioning of interstitial cells of Cajal by methylene blue and light leads to loss of slow waves. *Am J Physiol Gastrointest Liver Physiol* **266**: G485-G496.

Lorincz A, Redelman D, Horvath VJ, Bardsley MR, Chen H, and Ordog T (2008) Progenitors of interstitial cells of Cajal in the postnatal murine stomach. *Gastroenterol* **134**: 1083-1093.

Lowie BJ, Wang XY, White EJ, Huizinga JD (2011) On the origin of rhythmic calcium transients in the ICC-MP of the mouse small intestine. *Am J Physiol Gastrointest Liver Physiol* **301**: G835-G845.

Macfarlane GT and Macfarlane S (2012) Bacteria, colonic fermentation, and gastrointestinal health. *J AOAC Int* **95**: 50-60.

Malapaka RR, Khoo SK, Zhang J, Choi JH, Zhou XE, Xu Y, Gong Y, Li J, Yong EL, Chalmers MJ, Chang L, Resau JH, Griffin PR, Chen YE, and Xu HE (2012) Identification and mechanism of 10-carbon fatty acid as modulating ligand of peroxisome proliferator-activated receptors. *J Biol Chem* **287**: 183-195.

Malysz J, Thuneberg L, Mikkelsen HB, and Huizinga JD (1996) Action potential generation in the small intestine of W mutant mice that lack interstitial cells of Cajal. *Am Phys Soc* **34**: G387-G399.

Nakagawa T, Misawa H, Nakajima Y and Takaki (2005) Absence of peristalsis in the ileum of W/Wv mutant mice that are selectively deficient in myenteric interstitial cells of Cajal. *J Smooth Muscle Res* **41**: 141:151

Nutting DF, Kumar NS, Siddiqi SA, and Mansbach CM (2002) Nutrient absorption. *Curr Opin Gastroenterol* **18**: 168-75

Pistilli M (2012) Mechanisms underlying rhythmic activities of the gastrointestinal tract. *Unpublished Master of Science thesis*. McMaster University, Hamilton Canada.

Pluja L, Arberti E, Fernadez E, Mikkelsen HB, Thuneberg L, and Jimenez M (2001) Evidence supporting presence of two pacemakers in rat colon. *Am J Physiol Gastrointest Liver Physiol* **281**: G255-G266.

Olsson C and Holmgren S (2001) The control of gut motility. *Comp Biochem Physiol Part A Mol Integr Physiol* **128**: 479-501.

Robertson BE, Schubert R, Hescheler J, and Nelson MT (1993) cGMP-dependent protein kinase activates Ca-activated K channels in cerebral artery smooth muscle cells. *Am J Physiol Cell Physiol* **265**: C299-C303.

Salmhofer H, Neuhuber W. L. , Ruth P, Huber A, Russwurm M, and Allescher HD (2001) Pivotal role of the interstitial cells of Cajal in the nitric oxide signaling pathway of rat small intestine. *Cell Tissue Res* **305**: 331-340

Schemann M (2005) Control of gastrointestinal motility by the "gut brain" – the enteric nervous system. *J Pediatr Gastroenterol Nutr* **41**: S4-S6.

Shimizu Y, Matsuyama H, Shiina T, Takewaki T, and Furness JB (2008) Tachykinins and their functions in the gastrointestinal tract. *Cell Mol Life Sci* **65**: 295-311.

Smith TK, Reed JB, and Sanders KM (1987). Interaction of two electrical pacemakers in muscularis of canine proximal colon. *Am J Physiol Cell Physiol* **252**: C290-C299.

Stockinger S, Hornef MW, and Chassin C (2011) Establishment of intestinal homeostasis during the neonatal period. *Cell Mol Life Sci* **68**: 3699-3712.

Suzuki N, Prosser CL, and DeVos W (1986) Waxing and waning of slow waves in intestinal musculature. *Am J Physiol* **250**: G28-34.

Takeuchi H, Sekin S, Kojima K, and Aoyama T (2008) The application of medium-chain fatty acids: edible oil with a suppressing effect on body fat accumulation. *Asia Pac J Clin Nutr* **17**: 320-323.

Thuneberg L and Peters S (2001) Toward a concept of stretch-coupling in smooth muscle. I. Anatomy of intestinal segmentation and sleeve contractions. *Anat Rec* **262**: 110-124.

Torihashi S, Ward SM, Nishikawa S, Nishi K, Kobayashi S, Sanders KM (1995). c-Kit-Dependent development of interstitial cells and electrical activity in the murine gastorinetestinal tract. *Cell Tissue Res* **280**: 97-111.

Wang XY, Paterson C, and Huizinga J (2003) Cholinergic and nitrergic innervation of ICC-DMP and ICC-IM in the human small intestine. *Neurogastroenterol Motil* **15**: 531-543.

Wang XY, Vannucchi MG, Nieuwmeyer F, Ye J, Faussone-Pellegrini MS, and Huizinga JD (2005) Changes in interstitial cells of Cajal at the deep muscular plexus are associated with loss of distention-induced burst-type muscle activity in mice infected by Trichinella spiralis. *Am J Pathol* **167**: 437-453.

Wang XY, Aberti E, White EJ, Mikkelsen HB, Larsen JO, Jumenez M, and Huizinga JD (2009) $Igf1r^{+}/CD34^{+}$ immature ICC are putative adult progenitor cells, identified ultrastructurally as fibroblast-like ICC in Ws/Ws rat colon. *J Cell Mol Med* **13**: 3528-3540.

Ward SM, Baker SA, de Faoite A, Sanders KM (2003) Propagation of slow waves requires IP3 receptors and mitochondrial Ca2+ uptake in canine colonic muscles. *J Physiol* **549**: 207-218.

Ward SM, McLaren GJ, and Sanders KM. Interstitial cells of Cajal in the deep muscular plexus mediate enteric motor neurotransmission in the mouse small intestine. *J Physiol* **573**: 147-159.

Welch IM, Davison PA, Worlding J, and Read NW (1988) Effect of ileal infusion of lipid on jejunal motor patterns after a nutrient and nonnutrient meal. *Am J Physiol Gastrointest Liver Physiol* **255**:G 800-G806.

Won KJ, Sanders KM, and Ward S (2005). Interstitial cells of Cajal mediate mechanosensitive responses in the stomach. *Proc Natl Acad Sci USA* **102**: 14913-14918

Yoneda S, Takano H, Takaka M, and Suzuki H (2002) Properties of spontaneously active cells distributed in the submucosal layer of mouse proximal colon. *J Physiol* **542**: 887-897.

Yoneda S, Fukui H, and Takaki M (2004) Pacemaker activity from submucosal interstitial cells of Cajal drives high-frequency and low-amplitude circular muscle contractions in the mouse proximal colon. *Neurogastroenterol Motil* **16**: 621-627.

Zentek J, Buchheit-Renko S, Ferrara F, Vahjen W, Van Kessel AG, and Pieper R (2011) Nutritional and physiological role of medium-chain triglycerides and medium-chain fatty acids in piglets. *Anim Health Res Rev* **12**: 83-93.